THE JOURNAL OF PHYSICAL CHEMISTRY A
A JOURNAL OF THE AMERICAN CHEMICAL SOCIETY

pubs.acs.org/JPCA Article

Constraining the Effect of Surfactants on the Hygroscopic Growth of Model Sea Spray Aerosol Particles

Published as part of The Journal of Physical Chemistry virtual special issue "Advances in Atmospheric Chemical and Physical Processes".

Rachel L. Bramblett and Amanda A. Frossard*

Cite This: https://doi.org/10.1021/acs.jpca.2c04539 Read Online

ACCESS | Metrics & More | Article Recommendations | Supporting Information

ABSTRACT: The cloud condensation nuclei activation of sea spray aerosol (SSA) is tightly linked to the hygroscopic properties of these particles and is defined by their physical and chemical properties. While hygroscopic sea salt in SSA strongly influences particle water uptake, the marine-derived components that make up the organic fraction of SSA constitute a complex mixture, and their effect on hygroscopic growth is unknown. To constrain the effect of organic compounds and specifically surface-active compounds that adsorb on particle interfaces, particle hygroscopic growth studies were performed on laboratory-generated model sea salt/sugar particles. For sea salt/glucose particles, ionic surfactants facilitated water uptake at low relative humidity (RH), increasing the particle growth factor (GF) by up to 7.61%, and caused a reduction in the deliquescence relative humidity (DRH), while nonionic surfactants had a minimal effect. Replacing glucose with polysaccharide laminarin in sea salt/sugar/surfactant particles caused a reduction in GF at low RHs and minimized the effect of ionic surfactants on the DRH. At RHs above the DRH, the addition of anionic or nonionic surfactants caused a decrease in GF for both sea salt/glucose and sea salt/laminarin particles. The addition of cationic surfactants, however, did not have a dampening effect on water uptake of sea salt/sugar particles and even showed a GF increase of up to 3.7% at 90% RH. An increase in the complexity of the sugar dampens the water uptake for particles containing nonionic surfactants but increases the water uptake for cationic surfactants. The cloud activation potential for 100 nm particles analyzed in this study is higher for ionic surfactants and decreases with an increase in surfactant molecular size when particle interfacial tension is considered. The surfactant effect on the hygroscopic growth and cloud activation potential of the particles containing sea salt/sugar is dependent on the surfactant ionicity and molecular size, the particle size and interfacial tension, and the interactions between inorganic salt and organic species under different RH conditions.

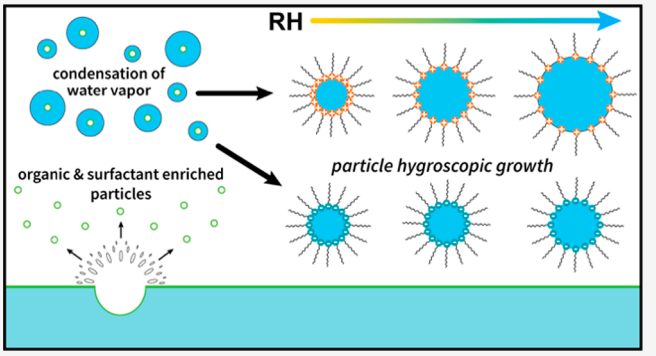

1. INTRODUCTION

The oceans cover over 70% of Earth's surface and produce one of the largest global fluxes of natural aerosol in the form of marine aerosol.[1,2] This aerosol is thus a large contributor to global climate and radiative forcing.[3,4] The total global flux of atmospheric sea salt particles is estimated to be 1.01×10^{13} kg year^{-1}, the majority of which are in the submicrometer size regime.[4,5] Primary marine aerosol particles, called sea spray aerosol (SSA), are directly emitted from the surface of the ocean.[1,2] SSA particles are produced at the ocean surface through the bubble bursting process, driven by breaking waves. Air bubbles entrained by breaking waves rise and, upon reaching the ocean−air interface, burst and collapse to eject SSA particles into the atmosphere.[1,6,7] Once in the atmosphere, SSA particles are rapidly aged through interactions with gas- and particle-phase species as well as interactions with solar radiation.[1,8] These particles can also absorb water vapor and grow into cloud droplets.[1,9−13]

SSA particles contain a large fraction of sea salt, depending on their size, and are thus hygroscopic and effective cloud condensation nuclei (CCN).[14−19] The water uptake of inorganic salts is dependent on their crystalline form, morphology, solubility, water activity, and ability to form hydrates.[1,20−24] However, SSA particles contain a fraction of organic compounds, which increases with decreasing particle

Received: June 29, 2022
Revised: October 20, 2022

Table 1. Chemical Constituents of Model Aerosol Particles and Their Relevant Properties, Including Molecular Structure, Molecular Weight, Density, Water Solubility, and Topological Polar Surface Area

classification	chemical compound	molecular structure	MW (g mol^{-1})	density (g cm^{-3})	water solubility	TPSA (Å^2)[i]
inorganic salt	NaCl	ions: Na^+, Cl^-	58.44	2.16[d]	35.8 g/100 mL[d]	0
	$MgCl_2$	ions: Mg^{2+}, Cl^-	95.21	2.32[d]	54.6 g/100 mL[d]	0
	sea salt	ions: Na^+, K^+, Ca^{2+}, Mg^{2+}, Cl^-, SO_4^{2-}, CO_3^{2-}	N/A	2.2[e]	soluble	0
saccharide	glucose	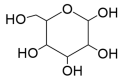	180.16	1.54[f]	soluble	110
	laminarin	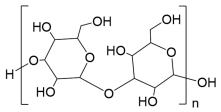	4400 – 4840[a]	1.5[g]	10 mg/mL[d]	269
anionic surfactant	sodium dodecyl sulfate (SDS)	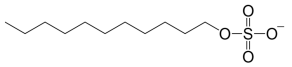	288.38	0.37[d]	1 g/10 mL[f]	74.8
	dioctyl sodium sulfosuccinate (AOT)	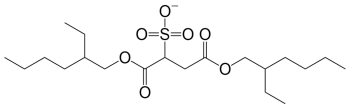	444.56	1.1[h]	14 g/L	118
cationic surfactant	cetyltrimethyl ammonium chloride (CTAC)	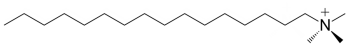	320.00	0.968[d]	440 mg/L[f]	0
	benzethonium chloride (Hyamine)	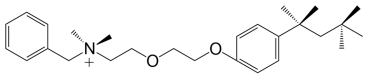	448.08	0.998[d]	100 mg/mL[d]	18.5
nonionic surfactant	polyethylene glycol tert-octylphenyl ether (Triton X-100)	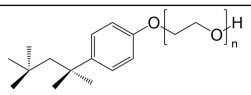	625 average[b]	1.07[d]	0.1 mL/mL[d]	29.5
	Tergitol NP-40	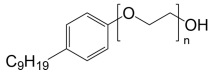	1960 average[c]	1.105[d]	soluble	N/A

[a]Variable degree of polymerization (n) ranging from 15 to 40.[117,118] [b]Average n ranging from 39 to 40. [c]Average n ranging from 9 to 10. [d]20–25 °C, Sigma-Aldrich. [e]From ref 1. [f]From ref 119. [g]From ref 120. [h]20–25 °C, Fisher Scientific. [i]References for topological polar surface area (TPSA) values are listed in the table, except for Tergitol NP-40, which is not listed (provided by PubChem, calculated using Cactvs 3.4.8.18).[119]

size[25,26] and directly influences their hygroscopicity.[27] Many organic compounds are not considered hygroscopic compared to salt, and several studies report growth factors (GFs) of up to only ~1.4 under a high relative humidity (RH) of 90%.[28−31] This organic fraction varies in composition depending on a number of factors, including ocean region, season, etc.[32−34] A recent wave tank experiment demonstrated that the hygroscopic growth of generated sea spray particles varied with the composition of the organic fraction of the particles, which in turn varied with the concentration of phytoplankton and bacteria.[35] Understanding how SSA particles interact with water vapor in the atmosphere is crucial to constraining their role in aerosol−cloud interactions, and the uncertainties related to these interactions remain a large contribution to the uncertainties in current climate models.[36]

The extent to which aerosol particles take up water is a function of the chemical and physical properties of the particle as well as the ambient humidity conditions. Specifically, water absorption is dependent on the particle composition, morphology, partitioning, size, and interfacial properties.[26,27,37−42] Kohler theory is often used to predict particle hygroscopic growth and the activation of CCN into cloud droplets, which takes into account two competing effects.[43] The solute effect, or Raoult effect, relates to particle composition and the decrease in saturation vapor pressure caused by solute within an aqueous droplet. The Kelvin effect corresponds to an increase in saturation vapor pressure due to the curvature of an aqueous droplet and is dependent on surface tension.[44] The combination of the two effects describes the supersaturation required to activate particles into cloud droplets.[43] The particle hygroscopic growth at high RH is associated with cloud condensation nuclei and indicative of cloud activation potential.[45,46]

Previous studies of SSA particle hygroscopic growth have largely focused on the hygroscopic properties of sea salt,[1,23,32,38] but the hygroscopicity of SSA, including ocean-derived organic compounds, has recently gained more attention.[35] Organic compounds have been shown to change the hygroscopic nature of salt and cause a decrease in hygroscopic growth.[15,47,48] Several studies have employed a humidified tandem differential mobility analyzer (HTDMA), which measures the ratio of particle size at a given RH to the dry particle size, to quantify hygroscopic properties by a hygroscopic growth factor.[49−54] Other studies have directly measured the change in particle size after humidification.[55−57] Some studies have also determined the hygroscopicity

https://doi.org/10.1021/acs.jpca.2c04539
J. Phys. Chem. A XXXX, XXX, XXX−XXX

parameter (κ) from measurements of CCN activation.[58−60] Additionally, computational model studies, including those using the AIM III model, which predicts the hygroscopic growth of particles of a given size and general composition, have shown that the addition of organic compounds reduces the hygroscopicity of salt particles.[48,61]

More recent studies are investigating the influence of the surfactant fraction of organic compounds observed in SSA on the particle hygroscopicity. Surfactants are surface-active compounds with polar headgroups and nonpolar tails that significantly reduce the surface tension of the interface at which they reside and can form into micelles. These surfactants have the ability to increase the CCN activity of aerosol particles and influence their ability to take up water.[42,62−65] This indicates that surfactants have the potential to influence particle hygroscopic growth. Surfactants have been observed to constitute a significant fraction of generated SSA and have been observed to represent 3% of the total particle mass of ambient aerosol particles.[66,67] Due to the large organic fractions observed in submicrometer SSA particles,[25,68,69] surfactants have more potential to significantly influence the role of SSA in cloud microphysics within the marine boundary layer, and thus, their role in particle hygroscopicity needs to be investigated. A recent review of surfactants outlines current understanding and measurements of surfactants in aerosol particles[70] and states that more work needs to be done to understand the influence of surfactants on the hygroscopic growth of atmospheric aerosol particles.

In this study, the influence of different surfactant compounds on the hygroscopic growth of model SSA particles was investigated. An HTDMA was used to measure the hygroscopicity of model SSA particles containing a single surfactant and compare the effects of surfactants varying across a range of surfactant classes and in particles of different dry sizes. The goal of this study was to better understand the role of surfactants in the hygroscopic behavior of SSA and how their properties affect both particle water uptake under subsaturated conditions and cloud activation potential. This was accomplished by measuring the hygroscopic growth of model SSA particles comprising a mixture of salt and organic compounds, a fraction of which were surfactants.

2. EXPERIMENTAL METHODS

2.1. Aerosol Particle Composition and Generation. Laboratory-generated aerosol particles were produced using an aerosol generation system (model 9200, Brechtel Manufacturing Inc.), which uses purified air to atomize aqueous solutions and generate aerosol particles. Solutions with a volume of 100 mL were made with ultrapure water (18.2 MΩ cm) and reagent-grade chemicals without additional purification. Each solution was mixed for 30 min with a stir plate and subsequently transferred to a solution fill bottle for atomization. All of the multicomponent solutions were made based on reagent mass ratios. It was assumed that the generated aerosol particles were internal mixtures reflecting the same composition and mass ratios of the reagent solutions. Atomizing and/or nebulizing are common methods to generate particles with mass ratios conserved from the bulk solutions.[71]

The model aerosol particle composition is based on the composition of SSA with sea salt as the inorganic fraction and sugar and a surfactant as a proxy for the SSA organic fraction.[66] Initial studies were done with single-component inorganic or organic particles and then on binary particles with a 2:1 inorganic to organic mass ratio to mimic the average composition of submicrometer SSA[34,72] in order to first understand the hygroscopic properties of single compounds and simple mixtures as a control and comparison to more complex mixtures. To study the influence of surfactants on particle water uptake, a fraction of the organic composition of the 2:1 sea salt/sugar particles was replaced with a single surfactant so that the particle organic composition was 90% sugar and 10% surfactant. Two standard surfactants per surfactant class (anionic, cationic, and nonionic) were investigated.

The properties of the particle components measured in this study are listed in Table 1. The inorganic compounds studied were magnesium chloride ($MgCl_2$) purchased from Sigma-Aldrich, sea salt purchased from Millipore, and sodium chloride (NaCl) purchased from Fisher Chemical. The organic compounds D-(+)-glucose (≥99.5%) and laminarin from *Laminaria digitata*, both purchased from Sigma-Aldrich, were used to represent the organic fraction of SSA. Glucose is a common organic compound found in seawater and has also been used as a primary marine aerosol tracer.[73,74] Laminarin is a polysaccharide of glucose found in most algae and phytoplankton and is a prolific marine carbohydrate that is significant in carbon cycling of the ocean.[75,76] Surfactant reagents were all purchased from Sigma-Aldrich and included the anionic surfactants sodium dodecyl sulfate (SDS) (≥99%) and dioctyl sulfosuccinate sodium salt (AOT) (≥97%), the cationic surfactants cetyltrimethylammonium chloride (CTAC) (25 wt % in water) and benzethonium chloride (Hyamine) (4 mM in water), and the nonionic surfactants Tergitol NP-40 (herein called Tergitol, 70% in water) and poly(ethylene glycol) *tert*-octylphenyl ether (Triton X-100, herein called Triton X).

2.2. Particle Hygroscopic Growth Measurements. Hygroscopic growth measurements were conducted on generated aerosol particles using a humidified tandem differential mobility analyzer (HTDMA) (BMI model 3100). The instrument specifications and methods of operation have been described previously by Lopez-Yglesias et al.[77] Briefly, generated aerosol particles were initially dried using an in-line diffusion drier and a subsequent Nafion drier to reach RH < 10%. The aerosol flow was then neutralized using an aerosol charge neutralizer (BMI model 9000) to ensure an equilibrium charge distribution. Dry aerosol particles with mobility diameters of 50, 100, or 300 nm were selected using a differential mobility analyzer (DMA) to create a monodisperse flow. The DMA transfer function is determined by the ratio of the sheath and sample flow rates[78] and is described in detail for this instrument by Lopez-Yglesias et al.[77] The monodisperse flow was then humidified through a Nafion humidifier to a specified RH (with an uncertainty of ±1% RH), and the resulting humidified particle size distribution was measured with a second DMA and a mixing particle condensation counter (MCPC) (BMI model 1720). In this study, the RH was increased in increments of 5% RH, starting at 50% or 70% RH, to measure the particle hygroscopic growth at a range of atmospherically relevant RHs and to capture the deliquescence RH (DRH) of NaCl-containing particles. The resulting number size distribution of the humidified particles at each RH set point was obtained.

A log-normal distribution was fit to each dry and humidified number size distribution, and the peaks for both dry and

https://doi.org/10.1021/acs.jpca.2c04539
J. Phys. Chem. A XXXX, XXX, XXX−XXX

humidified particle diameters were identified. All of the humidified size distributions for the different particle compositions exhibited a single mode, as shown in the example size distributions for 90% RH in Figure S1. The hygroscopic growth of each particle composition was quantified from the dry and humidified size distributions in the form of a hygroscopic growth factor (GF), which is defined as the ratio of the humidified particle diameter ($D_{p,wet}$) for a fixed RH to the dry particle diameter ($D_{p,dry}$), as shown in eq 1:

$$GF_{RH} = \frac{D_{p,wet}}{D_{p,dry}} \quad (1)$$

For ammonium sulfate particles measured with this instrument, the measured GFs lie within 3.5% of the value predicted by Kohler theory.[77]

The hygroscopic growth of the model SSA particles was determined for multiple dry particle sizes (50, 100, and 300 nm) and as a function of increasing RH (from 50% or 70% RH to 90% RH). For all particle compositions analyzed in this study, average hygroscopic GFs and standard deviations were obtained from four to six HTDMA scans of a single dry particle size for each RH set point.

The DRHs of particles containing inorganic salts were observed. Salts have a characteristic DRH, defined as the RH at which the water activities of the solid salt and the electrolyte solution are equal, above which point salt dissolution occurs.[21,79] This DRH is shown in hygroscopic growth curves by a sharp increase in water uptake at that RH.

For comparisons to hygroscopicity in other studies, κ was calculated from the GF at 90% RH (GF_{90}) using eq 2:

$$\kappa = 1 - GF^3 + \frac{(GF^3 - 1)}{RH} \exp\left(\frac{4\sigma M_w}{RT\rho_w D_d GF}\right) \quad (2)$$

where M_w is the molecular weight of water, R is the universal gas constant, T is the absolute temperature, ρ_w is the density of water, D_d is the dry particle diameter, and σ is the surface tension at the droplet−air interface.[80,81]

The surface tension used in the calculations was (i) the surface tension of pure water (72 mN/m) or (ii) the measured surface tension (as outlined in the Supporting Information). The κ determination allowed the cloud activation potential to be quantified by a critical supersaturation (S_c), defined as the supersaturation required for a particle to activate into a cloud droplet. S_c was calculated using eq 3:[82]

$$S_c = \exp\left(\sqrt{\frac{4A^3\sigma^3}{27T^3 D_d{}^3\kappa}}\right) \quad (3)$$

where $A = 8.69251 \times 10^{-6}$ K m^3 J^{-1}.[82] Particles with higher κ values have lower S_c and are thus more likely to be CCN.

2.3. Aerosol Particle Experiments. Particle hygroscopic growth, including GFs and DRH, were measured for a range of particle compositions, sizes, and RHs, as outlined here. Three sets of experiment types were completed and are outlined in Table S1, and the properties of the inorganic and organic components are outlined in Table 1. (i) Hygroscopic growth experiments were performed for single-component submicrometer particles to constrain the hygroscopic behavior of different individual constituents relevant to SSA. Using the single-component measurements, we can infer the contributions of different inorganic and organic compounds to the hygroscopic growth of the mixed two-component particles and the more complex systems. In these experiments, 100 nm particles containing NaCl, $MgCl_2$, sea salt, glucose, or SDS were generated. Sea salt particles were also generated at 50 and 300 nm for size comparisons. Measurements were taken over the range of 70−90% RH (except for sea salt particles, which had a range of 50−90% RH) at intervals of 5% RH, and four to six scans were completed at each RH set point. (ii) Two-component particles consisting of an inorganic salt and an organic compound (at a mass ratio of 2:1) were probed to observe the effects of different organic compounds on the water uptake of different salt particles in order to infer the contributions of different compounds in the more complex systems. In these experiments, 100 nm particles containing 2:1 sea salt/glucose, NaCl/glucose, $MgCl_2$/glucose, sea salt/laminarin, and sea salt/SDS mixtures were generated. Additionally, 50 and 300 nm particles with 2:1 sea salt/glucose and 2:1 sea salt/laminarin mixtures were also investigated. Measurements were taken over a range of 70−90% RH (except for sea salt/glucose particles, which had a range of 50−90% RH) at intervals of 5% RH, and four to six scans were completed at each RH set point. (iii) To probe the effect of surfactants on particle water uptake, including DRH and GF, 10% of the sugar fraction (glucose or laminarin) in the 2:1 sea salt/sugar particles was replaced with a single standard surfactant. Two surfactants from each of three different surfactant classes (anionic, cationic, and nonionic) were investigated. In these experiments, 50, 100, and 300 nm particles containing mixtures of sea salt and glucose with SDS, AOT, CTAC, Hyamine, Triton X, and Tergitol were generated with resulting sea salt/glucose/surfactant mass ratios of 2:0.9:0.1. Additionally, 50, 100, and 300 nm particles containing mixtures of sea salt and laminarin with SDS, AOT, CTAC, Hyamine, Triton X, and Tergitol were generated with resulting sea salt/laminarin/surfactant mass ratios of 2:0.9:0.1. Measurements were taken over a range of 50−90% RH, and four to six scans were completed at each RH interval. The GFs for each surfactant-containing particle experiment were compared to those of sea salt and 2:1 sea salt/sugar particles of the same particle sizes to constrain the effect of surfactants on GFs.

3. RESULTS AND DISCUSSION

3.1. Dependence of Single- and Two-Component Model SSA Particle Hygroscopic Growth on Particle Composition. *3.1.1. Single-Component Particles.* Here sea salt was investigated as the principal inorganic component of SSA, along with two other inorganic salts, NaCl and $MgCl_2$, which are the major components of sea salt.[1,57,83] The hygroscopic growth curves in Figure 1a show that the salts measured in this study are all inherently hygroscopic but have unique properties. From the HTDMA experiments, NaCl particles clearly show a DRH between 70 and 75% RH, reflecting the known DRH value at approximately 75% RH.[32] Meanwhile, the low DRH of $MgCl_2$ at 33% RH[38] is not observed in the range of RHs used in this study (Figure 1a). $MgCl_2$ creates stable hydrates and contains water even under very low RH conditions below its DRH.[1,83−85] The lower overall hygroscopic growth of $MgCl_2$ at high RHs (70% to 90% RH) is similar to that seen previously in hygroscopic studies of $MgCl_2$ particles.[83] Mg^{2+} has a higher charge density and disrupts hydrogen bonding between water molecules more than Na^+ does and influences the surface structure,[86] which

https://doi.org/10.1021/acs.jpca.2c04539
J. Phys. Chem. A XXXX, XXX, XXX−XXX

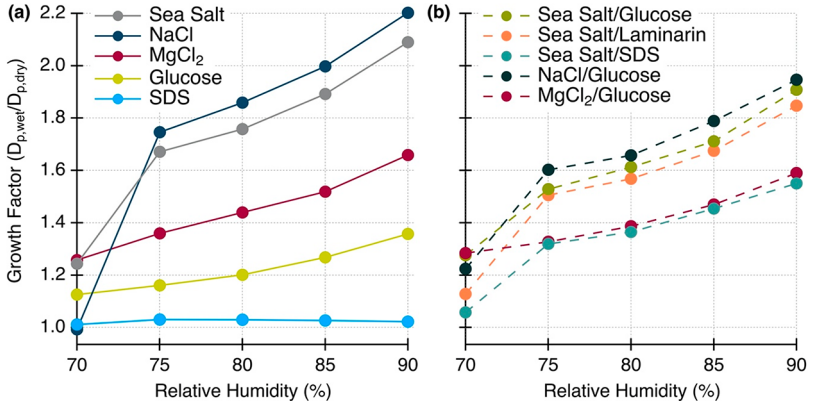

Figure 1. Hygroscopic growth curves for 100 nm (a) single-component and (b) two-component particles across a 70% to 90% RH range. Single-component particles (a) were generated from pure salts, glucose, or the anionic surfactant SDS. Two-component particles (b) were composed of 2:1 inorganic/organic internal mixtures. The error bars are smaller than the markers on this scale and thus are not included. The standard deviations for the GFs for the single-component particles at 90% RH are listed in Table 2, and those for the sea salt/glucose and sea salt/laminarin particles are listed in Table 3.

Table 2. Deliquescence Relative Humidity (DRH), Hygroscopic Growth Factor (GF), and Hygroscopicity Parameter (κ) Values at 90% RH for 100 nm Single-Component Inorganic and Organic Particles Compared to Those for Single-Component Particles Reported in the Literature

	DRH (%)		GF_{90}		κ	
single-component particle	other studies	exptl, this study	other studies	exptl, this study	other studies	exptl, calculated in this study
NaCl	73–77[a]	70–75	2.29[d]	2.20 ± 0.018	1.060[g]	1.179 ± 0.031
sea salt	73.5[b]	70–75	2.20[d]	2.09 ± 0.016	1.1[h]	0.995 ± 0.025
$MgCl_2$	30–35[c]	N/A	1.71[e]	1.66 ± 0.015	N/A	0.446 ± 0.015
glucose	N/A	N/A	1.37[f]	1.36 ± 0.017	0.14–0.20[i]	0.193 ± 0.012
SDS	N/A	N/A	N/A	1.02 ± 0.004	0.133[g]	0.009 ± 0.002

[a]From refs 1, 32, 88, 121, and 122. [b]From refs 1 and 23. [c]From refs 83, 88, and 122. [d]From ref 23. [e]From ref 38. [f]From ref 31. [g]From ref 64. [h]From ref 23. [i]From refs 92 and 123.

could directly impact water adsorption. The DRH of salts has been well-studied, and the experimental results for particles containing only inorganic salts in this study closely align with those of particle growth experiments previously conducted on inorganic salts[1,23,38,87,88] (Table 2). One recent study observed that water vapor may deposit on NaCl particles under very low RH conditions, thus impacting its apparent DRH.[89] Additionally, the κ values calculated from the GFs for NaCl (0.179 ± 0.031) and sea salt (0.995 ± 0.025) in this study are very similar to those calculated in previous studies (1.060[64] and 1.1,[23] respectively) (Table 2).

The DRH of sea salt is also between 70 and 75% RH, similar to that of NaCl (Figure 1a). Since the composition of sea salt is a mixture of inorganic salts, not just NaCl, the deliquescence and hygroscopic growth change due to the presence of salts containing Ca^{2+} and Mg^{2+}, which have lower DRH values and different hygroscopic properties than those containing Na^+ and Cl^-.[23,32,83] This is demonstrated by the higher GFs of NaCl particles compared to those of sea salt particles at RHs of 75% and above (Figure 1a).

Figure 1a shows the clear difference in hygroscopic growth between particles composed of sea salt, NaCl, and $MgCl_2$. The overall extent of water uptake by the $MgCl_2$ particles (GF = 1.66 at 90% RH) is considerably less than that of NaCl particles (GF = 2.20 at 90% RH). The resulting hygroscopic growth of sea salt reflects the mixture of these two salts. Sea salt acts as a mixed particle, and thus, its hygroscopicity is more complicated. This can be attributed to the potential presence of partially deliquesced states depending on the RH conditions.[21,32] Interfacial studies on marine aerosol have also shown that the air–particle interface is rich in Mg^{2+} and Cl^- ions, with divalent Mg^{2+} shown to significantly impact the water surface structure.[86,90] These surface properties therefore could also contribute to the discrepancies between the hygroscopic behaviors of NaCl and sea salt. Because NaCl is the principal salt in dried sea salt, the hygroscopicity of sea salt particles follows a trend more similar to that of the NaCl particles than that of the $MgCl_2$ particles. The hygroscopic growth curve of sea salt, however, has key differences from that of NaCl (Figure 1a). At 70% RH, prior to deliquescence, the sea salt particles have greater water uptake than pure NaCl particles and show the same GF as $MgCl_2$ particles at the same RH. $MgCl_2$ controls the initial hygroscopic behavior of sea salt,[91] as demonstrated in this study with the GF agreement of sea salt and $MgCl_2$ at 70% RH. Also, the extent of sea salt particle water uptake at RHs above the DRH is less than that of NaCl, with a GF of 2.09 at 90% RH.

The hygroscopic behavior of particles containing glucose or surfactant SDS is clearly differentiated from that of the salt particles, with no clear phase transition of deliquescence and much less water uptake from 75% to 90% RH (Figure 1a), as has been previously demonstrated.[29,92] The GFs of particles containing pure glucose or pure SDS are much lower than those of the pure salt particles at high RH. At 70% RH, however, glucose particles have a higher GF and more water uptake than pure NaCl particles, which have not yet reached deliquescence (Figure 1a). This shows that at RHs below the DRH of NaCl, glucose particles retain more water than pure

https://doi.org/10.1021/acs.jpca.2c04539
J. Phys. Chem. A XXXX, XXX, XXX–XXX

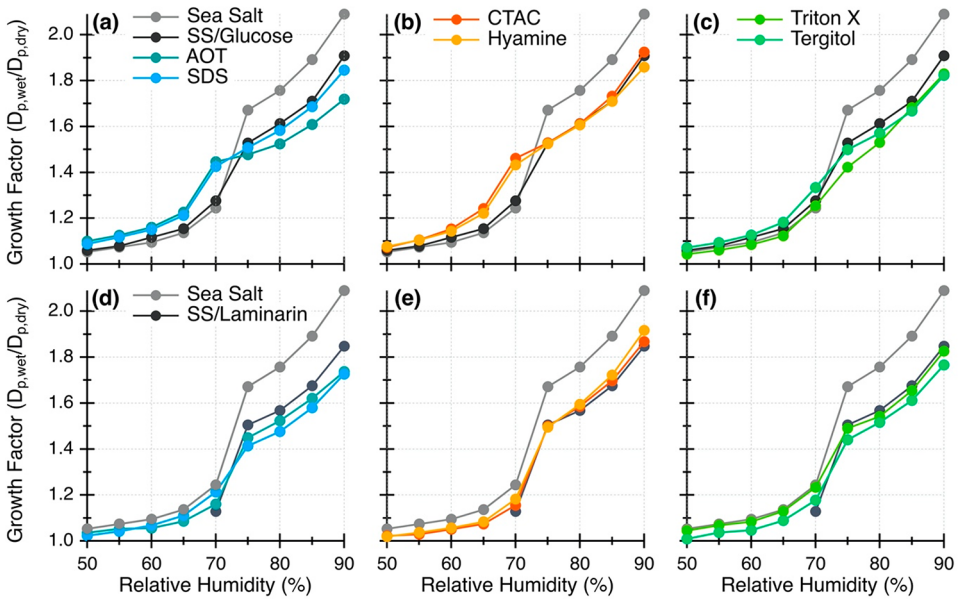

Figure 2. Hygroscopic growth curves of 100 nm sea salt particles with additions of sugar and a surfactant from 50% to 90% RH. The curve for pure sea salt (gray) is shown in each panel for reference. (a–c) Ternary sea salt/glucose/surfactant particles (2:0.9:0.1) with (a) the anionic surfactants AOT and SDS, (b) the cationic surfactants CTAC and Hyamine, and (c) the nonionic surfactants Triton X and Tergitol are compared to sea salt and sea salt/glucose (2:1). (d–f) Ternary sea salt/laminarin/surfactant particles (2:0.9:0.1) with (d) AOT and SDS, (e) CTAC and Hyamine, and (f) Triton X and Tergitol are compared to sea salt and sea salt/laminarin (2:1). All of the curves are shown from 50% to 90% RH, except those for the particles with the two-component sea salt/laminarin mixtures (2:1), which range from 70% to 90% RH. The error bars are smaller than the markers on this scale and thus are not included. The standard deviations for the GFs at 90% RH are listed in Table 3.

NaCl particles. The pure glucose particles have GFs larger than 1.0 across the RH range studied, which increase to almost 1.4 at 90% RH and match previous HTDMA studies performed on glucose particles[30,31] (Table 2). The hygroscopic behavior of sugars has been linked to water solubility and oxidation state,[93] and previous measurements have demonstrated that glucose particles are somewhat hygroscopic,[92,94] with κ values of 0.14–0.20[92] (Table 2). The κ for glucose calculated in this study falls within that range (κ = 0.193 ± 0.012 at 90% RH; Table 2). SDS particles maintain GFs very close to 1.0 for all RHs, indicating minimal to no water uptake (Figure 1a). This aligns with previously reported results for SDS nanoparticles showing that particles composed of this surfactant alone are not hygroscopic and maintain GFs less than 1.02 from 5% to 95% RH.[29] Additionally, previous CCN measurements showed κ for SDS particles to be 0.133.[64] The κ value in this study is even lower (0.009 ± 0.002) when a surface tension of 72 mN/m is assumed (Table 2). On the other hand, CCN measurements of C_8–C_{14} fatty acid sodium salts demonstrated increased CCN potential, attributed to a reduction in surface tension and surfactant partitioning.[95] The GF and κ values for SDS particles further demonstrate the importance of including reliable surface tension values in calculations of κ.

3.1.2. Two-Component Inorganic–Organic Particles. The addition of an organic compound to a salt particle dampens the extent of rapid growth occurring at the DRH of the salt particle and decreases the particle GFs at high RHs (Figure 1b). While the DRHs of sea salt and NaCl particles containing organic compounds still lie between 70% and 75%, the slope of the curve is decreased with the addition of glucose or laminarin (Figure 1b). Similarly, previous studies observed decreases in the DRH of salt upon the addition of organic compounds.[27,29,96–98]

The GFs of mixed sea salt and glucose particles are dependent on their organic fraction, with GFs decreasing as the fraction of glucose increases, at RHs above the DRH (Figure S2 and Text S1). Below the DRH, the trend in GFs with organic fraction is less clear (Figure S2). In sea salt particles, when the fraction of glucose is ≥0.5, the characteristic spike in GF at the DRH of sea salt disappears (Figure S3). A similar trend was observed in previous studies with NaCl/SDS particles, where the DRH of the salt was not observed once the organic fraction surpassed the inorganic salt fraction.[29] However, the salt still facilitates hygroscopic growth as mixed salt/organic particles have higher GFs than organic-only particles (Figures S2 and S3).[29]

The hygroscopic growth of sea salt particles at RHs above the DRH is reduced with the addition of organic compounds (Figure 1). The sea salt GF at 75% RH is reduced by 8.6% and 9.9% with the addition of glucose and laminarin, respectively. The sea salt/laminarin particles exhibit lower hygroscopic growth than the sea salt/glucose particles across the 70% to 90% RH range. Lower hygroscopic growth of complex sugar particles compared to simple sugar particles has been observed previously across a wider RH range and was linked to the higher molecular weights of complex sugars.[93,99] An increase in molecular weight and the number of glucose units has been tied to an increase in sugar solubility,[100,101] which highlights solubility as a determining factor in the hygroscopic growth of sugars.

Similar to sea salt particles, the NaCl particle hygroscopic growth decreases above the DRH with the addition of glucose (Figure 1). At 75% RH, the NaCl particle GF is reduced by 8.2% with the addition of glucose. A similar decrease in hygroscopicity was observed in NaCl particles with an increase in fulvic acid fraction.[58] The addition of glucose has the least impact on the hygroscopic growth of $MgCl_2$ particles. Glucose

https://doi.org/10.1021/acs.jpca.2c04539
J. Phys. Chem. A XXXX, XXX, XXX–XXX

lowers the particle GF by only 2.4% at 75% RH when added to $MgCl_2$ particles. Because $MgCl_2$ particles are more hygroscopic at lower RHs (<75%) and less hygroscopic at high RHs (>75%) compared to the other salt particles, the addition of a less hygroscopic organic compound does not have as significant of a dampening effect on $MgCl_2$ as it does on NaCl or sea salt.

The hygroscopic growth of organic compounds in mixed aerosols has also been linked to the particle mixing state and organic coating thickness.[102,103] In the presence of salt, sugars can form an organic shell around the salt core, and the composition of the organic coating will determine the water uptake.[93,99] Previous studies have shown that in core−shell particle morphologies, organic shells may suppress the uptake of water by hindering water diffusion to the inorganic core, but this does not occur for all core−shell particles.[52,104] The effect of the organic compound on the salt particle water uptake is dependent on the organic composition and specifically linked to the solubility of the organic compound, which may vary in an ionic environment[96−98,101] such as an aqueous salt particle.

The water uptake by sea salt particles is even more drastically decreased by the addition of the anionic surfactant SDS, which reduces the GF by 21% at 75% RH (Figure 1b). The substitution of glucose by SDS in sea salt particles results in an 18% decrease in overall particle GF at 90% RH compared to sea salt alone. This large decrease in sea salt particle GFs was not observed with the addition of glucose or laminarin (Figure 1b), indicating that the surfactant properties contribute more to the observed GFs than just molecular weight. Previously it was observed that an increase in the number of SDS monolayers in NaCl nanoparticles, which depends on the amount of SDS present in the particle, decreased the hygroscopic growth and DRH of NaCl particles.[29] SDS decreases the particle surface tension, which influences the phase transition of salt, affects gas-to-particle condensation, and allows water adsorption onto a NaCl/SDS particle to occur at lower RH than that of a pure NaCl particle.[29] The addition of SDS to NaCl also influences particle critical supersaturation, with an increasing SDS relative mass fraction corresponding to a decrease in S_c.[105] Even in smaller amounts, SDS caused an increase in particle CCN activity since the influence on the surface tension (the Kelvin effect) overrides the competing solute effect.[106]

When the particle composition reflects an internal mixture of both inorganic and organic components, the expected hygroscopic growth of a particle becomes less clear. Several studies have investigated how these internal mixtures can lead to core−shell morphologies in aerosol particles and how the organic shell influences interfacial processes, including water uptake and adsorption into a particle.[103,104]

3.2. Surfactant Properties Influence the Hygroscopicity of 100 nm Mixed Sea Salt/Sugar/Surfactant Particles. Figure 2 compares the hygroscopic growth curves of the ternary particles to those of sea salt only and 2:1 sea salt/sugar particles. Trends in the effect of surfactants on the hygroscopic growth of these model particles emerge based on the class and properties of surfactant present in the particle.

3.2.1. Surfactant Influence on Sea Salt/Glucose Particles. The addition of ionic surfactants (both anionic and cationic) leads to enhanced water uptake in sea salt/glucose particles under RH conditions below the DRH (Figure 2a,b). For sea salt/glucose particles containing ionic surfactants, there is a 2.6% and 3.8% increase in GFs at 50% RH with the addition of SDS and AOT, respectively. Similarly, there is a 1.2% and 1.6% increase in GFs for sea salt/glucose particles containing CTAC and Hyamine, respectively. At 65% RH, the increases in GFs compared to pure sea salt/glucose particles are amplified, as shown by the 4.9% and 6.2% increases in GFs for particles containing SDS and AOT, respectively, and the 7.6% and 5.7% increases in GFs for particles containing CTAC and Hyamine, respectively. At this RH, particles are closely approaching deliquescence, and enough water has adsorbed onto the particles to allow surfactants to dissolve. Since at this RH (prior to the DRH) the particles still maintain a smaller size and thus a large surface-to-volume ratio, surfactants can more easily adsorb to and envelop the particle surface, in turn lowering the particle surface tension and causing the measured increase in hygroscopic growth.

The DRH of sea salt/glucose particles also shifts to a lower RH with the addition of an ionic surfactant (Figure 2a,b). The DRH of pure sea salt/glucose particles falls between 70% and 75%, whereas sea salt/glucose particles with the addition of both the anionic and cationic surfactants have DRHs between 65% and 70%, as shown in the hygroscopic growth curves by the sharp increase in growth between these RHs (Figure 2a,b). This shift of DRH to lower RH was also observed in hygroscopic studies of NaCl/AOT and NaCl/SDS nanoparticles when surfactants created a single surface monolayer.[29,97,98] This shows that ionic surfactants can increase the hygroscopic growth of particles containing salt at lower RHs, which could increase water exposure to the salt particle fraction, facilitating deliquescence at a lower RH than that of salt alone.

Unlike the ionic surfactants, the nonionic surfactants have a smaller effect on sea salt/glucose water uptake. The addition of nonionic surfactants has a minimal effect on the water uptake of sea salt/glucose particles under RH conditions below the DRH (Figure 2c). The GFs for sea salt/glucose particles containing nonionic surfactants at these lower RHs do not deviate much from the GFs of sea salt/glucose only particles. The addition of nonionic surfactants also has a less pronounced shift in the DRH and less pronounced increase in growth at the DRH (Figure 2c) compared to the DRH of sea salt/glucose particles with ionic surfactants (Figure 2a,b). The sea salt/glucose particles with nonionic surfactants appear to have a more gradual deliquescence occurring over a range of RHs (65% to 75% RH) rather than the spontaneous deliquescence at a single distinctive RH typically seen for salt particles. This could imply that the presence of a nonionic surfactant decreases the rate of salt deliquescence in aqueous sea salt/glucose particles. Nonionic surfactants have been shown to be incorporated into the crystalline structure of salt,[107] which could explain the unique deliquescence behavior of sea salt/glucose particles containing nonionic surfactants.

This difference in behavior across surfactant types at RHs less than the DRH demonstrates that the ionic charge of a surfactant may affect the initial adsorption of water onto sea salt/glucose particles. Specifically, there is an increase in water uptake (increase in GFs) from 50% to 70% RH for sea salt/glucose particles containing surfactants with charged headgroups that is not observed with the addition of nonionic surfactants. The adsorption of ionic surfactants at an interface is enhanced in the presence of salt.[108] Electrolytes in solution may shield repulsions between the charged polar headgroups of ionic surfactants, allowing for denser surfactant packing at an interface.[108,109] This compact surfactant packing can lead to

https://doi.org/10.1021/acs.jpca.2c04539
J. Phys. Chem. A XXXX, XXX, XXX−XXX

a decrease in interfacial tension.[108] Since sea salt includes salts that form stable hydrates and deliquesce at low RH, such as $MgCl_2$, dissociated ions could exist in aqueous droplets below the observed DRH. This means that below the DRH of sea salt/glucose particles, electrolyte shielding could occur and allow for more adsorption of ionic surfactants at the particle surface. This could have larger implications at low RH since lower particle water content and overall particle surface area could allow for complete saturation of the particle surface with a surfactant monolayer, lowering the interfacial tension and thus causing the observed enhanced GFs below the DRH.

At high RH (above the DRH), the change in GFs of sea salt/glucose particles due to the addition of surfactants varies based on the surfactant type but does not show the clear trend between the addition of ionic and nonionic surfactants demonstrated at lower RHs (Figure 2). The addition of nonionic surfactants to sea salt/glucose particles decreases water uptake and GFs from 75% to 90% RH (Figure 2c). This same trend is observed with the addition of anionic surfactants to sea salt/glucose particles, with a considerable impact on water uptake by the addition of AOT (Figure 2a).

The largest decrease in GF at high RH is due to the addition of AOT in the sea salt/glucose particle. Compared to sea salt/glucose, the addition of AOT suppresses the GF by 9.9% at 90% RH. The decrease in growth at RHs above the DRH has previously been shown in HTDMA studies of NaCl/AOT particles.[97] This enhanced suppression could be due to steric hindrance at the particle interface, since AOT is the only surfactant in this study with a dual hydrophobic tail (Table 1). In simulations studying interfacial properties of single- and double-tailed surfactants, double-tailed surfactants were shown to be less efficient and require a higher bulk concentration to achieve the same surfactant concentration at an interface.[110] Consequently, aqueous particles containing AOT could have higher surface tension, which combined with steric hindrance on the surface could negatively interfere with water adsorption compared to particles containing single-tailed surfactants, such as SDS.

Sea salt/glucose particles containing cationic surfactants show the least deviation in hygroscopic growth from sea salt/glucose only particles at RHs above the DRH (Figure 2b). The particles containing CTAC show a slightly enhanced GF (increase of 0.9%) compared to the GF of sea salt/glucose particles at 90% RH. This slight increase may be caused by the electrolyte shielding discussed in the previous section. This would reduce the particle interfacial tension and increase the hygroscopic growth. However, this increase may also be attributed to instrument noise due to less stable RH measurements at 90% RH.

At high RHs, there is a clear difference in the effects on hygroscopic growth caused by the addition of nonionic and anionic surfactants compared to the addition of cationic surfactants to sea salt/glucose particles. It is possible that the cationic surfactants dissolve more into the bulk of the aqueous particle at high RHs and thus do not contribute to a further decrease in hygroscopicity of sea salt/glucose particles beyond the decrease due to glucose. Additionally, the difference between the cationic surfactants and nonionic surfactants may be due to the ability of nonionic surfactants to be integrated into salt crystals when the particles were dried.[107] This could change the properties of the crystalline salt and its deliquescence, which could alter the water uptake of the particles as they were humidified past the DRH.

Overall, there is a discernible difference in the effects on sea salt/glucose particle hygroscopicity caused by the addition of surfactants depending on whether the RH is below or above the DRH (Figure 2). Below the particle DRH, the addition of anionic and cationic surfactants increases the GFs of sea salt/glucose particles, while the addition of nonionic surfactants has a minimal effect. This increase in hygroscopic growth could be attributed to a significant decrease in surface tension caused in the presence of salt by anionic and cationic surfactants forming charged monolayers.[111] Above the DRH, the addition of anionic and nonionic surfactants decreases the particle GFs, while the cationic surfactants have little to no effect. At RHs above the DRH, the particle growth and surface area are larger, so the surfactant fraction may no longer be sufficient to saturate the particle surface or lower the interfacial tension of sea salt/glucose particles enough to facilitate an increase in particle hygroscopic growth. The depression in sea salt/glucose particle GFs observed at RHs above the DRH with the addition of anionic and nonionic surfactants can be attributed to the decrease in hygroscopicity of the mixtures when the surfactants are dissolved in the bulk of the particle.

The values of κ and S_c for the various particle compositions, shown in Figure 3 and outlined in Table 3, demonstrate the differences in the cloud activation potentials of sea salt/glucose particles when considering the surface tension effects caused by different surfactants. When a droplet−air surface tension equal to that of pure water (ST_{water}) is assumed for surfactant-containing particles (Figure 3a), the S_c remains at or above that of the mixed sea salt/glucose only particles. This is because the differences in calculated S_c between different particle compositions are driven solely by differences in the measured hygroscopic GFs (eqs 2 and 3). Based on the ST_{water} assumption, the addition of surfactants to sea salt/glucose particles causes a decrease in the CCN potential.

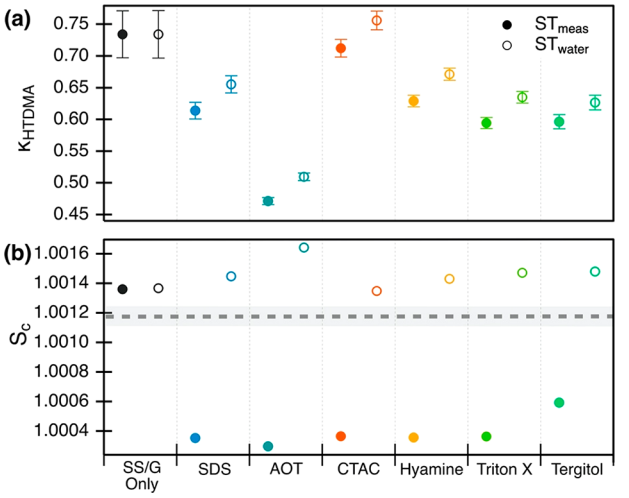

Figure 3. Calculated (a) κ and (b) S_c values for 100 nm diameter particles containing sea salt and glucose with the addition of the individual surfactants. Open markers used a surface tension of 72 mN/m in the calculations, while solid markers used the measured surface tensions. The dashed line and shading in (b) indicates the calculated S_c and standard deviation for pure sea salt particles.

To better represent the particle surface tension, the measured surface tensions (ST_{meas}) of bulk sea salt/glucose/surfactant (2:0.9:0.1 mass ratio) solutions for the particle surfactant concentrations were used to determine S_c from κ

https://doi.org/10.1021/acs.jpca.2c04539
J. Phys. Chem. A XXXX, XXX, XXX−XXX

Table 3. Hygroscopic Growth Factors at 90% RH (GF_{90}), Hygroscopicity Parameters (κ), and Critical Supersaturations (S_c) for 100 nm Sea Salt Particles Containing Each Organic Compound Listed[a]

		sea salt/glucose					sea salt/laminarin		
surfactant class	standard organic	GF_{90}	κ_{90} (ST_w)	κ_{90} (ST_m)	S_c (ST_w)	S_c (ST_m)	GF_{90}	κ_{90} (ST_w)	$S_{c,90}$ (ST_w)
N/A	sugar only	1.908 ± 0.028	0.734 ± 0.028	0.734 ± 0.037	1.0014	1.0014	1.848 ± 0.012	0.657 ± 0.015	1.0014
anionic	SDS	1.846 ± 0.011	0.656 ± 0.011	0.614 ± 0.013	1.0015	1.0004	1.727 ± 0.010	0.517 ± 0.011	1.0016
	AOT	1.720 ± 0.006	0.510 ± 0.006	0.471 ± 0.006	1.0016	1.0003	1.737 ± 0.008	0.528 ± 0.009	1.0016
cationic	CTAC	1.925 ± 0.011	0.756 ± 0.011	0.712 ± 0.014	1.0013	1.0004	1.868 ± 0.012	0.682 ± 0.016	1.0014
	Hyamine	1.859 ± 0.008	0.671 ± 0.008	0.629 ± 0.009	1.0014	1.0004	1.917 ± 0.006	0.745 ± 0.007	1.0014
nonionic	Triton X	1.830 ± 0.008	0.635 ± 0.008	0.628 ± 0.008	1.0015	1.0004	1.826 ± 0.008	0.631 ± 0.010	1.0015
	Tergitol	1.823 ± 0.010	0.627 ± 0.010	0.597 ± 0.011	1.0015	1.0006	1.766 ± 0.022	0.561 ± 0.025	1.0016

[a]Particle compositions are sea salt/sugar (2:1) without surfactants or sea salt/sugar/surfactant (2:0.9:0.1) for both sugars (glucose and laminarin). Calculated κ values are reported as mean ± standard deviation. The two surface tensions used are the surface tension of pure water (ST_w = 72 mN/m) and the measured surface tension (ST_m).

(Figure 3b). The measured surface tensions are listed in Table S2 and shown in Figure S4, and the particle surfactant concentrations are listed in Table S3. When the unique surface tension of each composition is considered in the S_c determination, the CCN potential of each surfactant-containing particle increases, as demonstrated by a 0.09% to 0.13% decrease in S_c. For example, sea salt/glucose/AOT particles had the largest S_c under the ST_{water} assumption, but they have the lowest S_c when ST_{meas} is considered. Comparison across the different surfactant classes shows that the sea salt/glucose particles containing ionic surfactants have lower S_c values than particles containing nonionic surfactants when ST_{meas} is used. This difference in S_c with surfactant ionic class could be a result of the salting-out effect observed previously with NaCl particles containing Triton X. In the presence of salt, a higher concentration of Triton X is required to decrease the surface tension.[71] The S_c for sea salt/glucose particles containing Tergitol is distinctly higher than those for the other particle compositions, and these particles also consequently have the largest molecular size. Further studies of the effect of surfactant size on hygroscopic growth and particle activation of mixed salt/organic particles are needed to better constrain this trend in surfactant ionicity and molecular size with particle critical supersaturation.

3.2.2. Surfactant Influence on Sea Salt/Laminarin Particles. The addition of surfactants to sea salt/laminarin particles does not show a perceptible change in the particle DRH, indicating that the surfactants have little, if any, influence on the DRH of sea salt/laminarin particles (Figure 2d–f). The DRH values of sea salt/laminarin particles containing surfactants still fell between 70% and 75% RH, like those of pure sea salt and sea salt/laminarin particles. The addition of laminarin to sea salt particles does decrease the slope of the GF spike of sea salt at the DRH, but the addition of surfactants to those sea salt/laminarin particles showed no significant further decrease (Figure 2d–f). The slopes at the DRH for particles with the addition of anionic and nonionic surfactants appear to be slightly but not significantly depressed compared to that of sea salt/laminarin particles (Figure 2d–f).

At RH values less than the DRH, all sea salt/laminarin particles containing surfactants have lower GFs than pure sea salt particles (Figure 2d–f). The GFs of sea salt/laminarin particles without surfactants were not measured in the range of 50 to 70% RH, but this still shows that at lower RHs (below the DRH), the laminarin/surfactant mixture decreases the GFs of pure sea salt. While the sea salt/laminarin/Triton X particle growth curve from 50 to 70% RH aligns closest to that of sea salt particles, it still exhibits a 0.6% to 1% decrease in GF from that of pure sea salt over this RH range. The decrease in GFs below the DRH for sea salt/laminarin particles containing surfactants is likely due to the partitioning of laminarin to the particle surface where it can form a shell and block particle water uptake, as will be discussed in the next section.

At 70% RH, right before the DRH of these particles, an increase in water uptake is observed for all sea salt/laminarin/surfactant particles compared to that of the sea salt/laminarin particles (Figure 2d–f). Under these conditions, enough water vapor is present to solubilize the laminarin in the particles, or break up the shell structure of the laminarin, and the adsorbed water can reach the salt core. The sea salt can then begin to rapidly take up water as the conditions approach and reach the DRH. At this point, surfactants in the now aqueous particle can partition to the particle surface, lower the interfacial tension, and increase hygroscopic growth. The addition of the anionic surfactants SDS and AOT causes increases of 7.5% and 2.8%, respectively, in GFs of sea salt/laminarin at 70% RH. The addition of cationic surfactants CTAC and Hyamine causes 2.4% and 4.8% increases, respectively, in sea salt/laminarin particle GFs at 70% RH. The addition of the nonionic surfactants Triton X and Tergitol also causes notable increases of 9.3% and 4.3%, respectively, in the GFs of sea salt/laminarin at 70% RH.

The largest difference in the GF curves of sea salt/laminarin particles with the addition of surfactants is observed at RHs greater than the DRH. At these RHs, the hygroscopic growth behavior of the sea salt/laminarin/surfactant particles deviates from the hygroscopic growth of sea salt/laminarin particles in unique ways depending on the type of surfactant added. Table 3 details the GF at 90% RH for these particle compositions. Sea salt/laminarin particles containing anionic or nonionic surfactants show a decrease in hygroscopic growth compared to sea salt/laminarin only particles. Sea salt/laminarin particles containing the anionic surfactants SDS and AOT decrease the GFs at 90% RH by 6.6% and 6.0%, respectively. The addition of the nonionic surfactants Triton X and Tergitol reduce the GFs of sea salt/laminarin particles at 90% RH by 1.2% and 4.4%, respectively. However, the addition of the two cationic surfactants CTAC and Hyamine causes increases of 1.1% and 3.7%, respectively, in the GFs of sea salt/laminarin particles at 90% RH. The S_c values calculated from the 90% RH GFs for sea salt/laminarin/surfactant particles are within 0.02% for all of the surfactant-containing particles when it is assumed that

https://doi.org/10.1021/acs.jpca.2c04539
J. Phys. Chem. A XXXX, XXX, XXX−XXX

the particle surface tension is that of pure water (Table 3). While particles containing cationic surfactants exhibit a slightly improved CCN activation potential based on a lower S_c, the CCN activation potentials of all sea salt/laminarin particles are comparable (Table 3). The CCN activity of sea salt/laminarin/surfactant particles, however, would be better constrained with a measured particle surface tension for each unique composition.

In sea salt/laminarin particles, the presence of the large polysaccharide significantly decreases the extent of water uptake of sea salt from 70% to 90% RH and even more so above the DRH, reducing the GF by 9.9% to 11.6% from that of sea salt only. Below the DRH (RH < 75%), all of the surfactants appear to slightly increase the hygroscopic growth compared to the GF of sea salt/laminarin only particles at 70% RH. The addition of nonionic and anionic surfactants causes the largest increases in GF at 70% RH, with SDS and Triton X additions causing the GF to approach that of sea salt only. Under humid conditions (>75% RH), however, nonionic and anionic surfactants further decrease the hygroscopic growth of sea salt/laminarin particles. Cationic surfactants, on the other hand, cause minimal change in hygroscopic growth from 70% to 90% RH compared to sea salt/laminarin only particles but do slightly enhance water uptake at high RHs.

3.2.3. Comparison of Surfactant Influence on Sea Salt/Glucose and Sea Salt/Laminarin Particles. The most apparent difference in the hygroscopic growth curves of sea salt/laminarin/surfactant particles compared to those of sea salt/glucose/surfactant particles is that across all surfactant classes, the sea salt/laminarin/surfactant particles show a sharp increase in growth at the DRH, similar to that of sea salt only particles (Figure 2). As discussed earlier, the slopes of the GF curves at the DRH for the sea salt/glucose/surfactant particles were all suppressed compared to those of pure sea salt particles (Figure 2). This decrease in slope occurs because surfactants facilitate water uptake below the DRH, which was not observed in sea salt/laminarin/surfactant particles, and decrease water uptake above the DRH. The intensity of growth at the DRH is thus perceived to be reduced compared to that of sea salt/laminarin/surfactant particles. Additionally, based on these experiments, the DRH of the sea salt/laminarin/surfactant particles shows no perceptible change from those of sea salt or sea salt/laminarin, which lie between 70% and 75%, unlike the lower DRH shown for sea salt/glucose/ionic surfactant particles (Figure 2).

At RHs less than DRH, the GFs for sea salt/laminarin/surfactant particles are less than those of sea salt/glucose/surfactant particles (Figure 2). This is also shown in the steeper slopes of the GF curves from 50% to 65% RH for the sea salt/glucose/surfactant particles (Figure 2). The ratios of particle GF at 65% RH to the GF at 50% RH range from 1.08 to 1.16 for sea salt/glucose/surfactant particles and from 1.05 to 1.09 for sea salt/laminarin/surfactant particles. Comparing these ratios to that of sea salt only particles (1.08) indicates that the replacement of glucose with laminarin further suppresses the water uptake of sea salt particles at low RHs from 50% to 65% RH.

Under low RH conditions, sea salt/glucose/surfactant particles show enhancement of water uptake compared to sea salt only particles (increased GFs), while sea salt/laminarin/surfactant particles have depressed particle water uptake compared to sea salt only particles (decreased GFs). Laminarin is a much larger molecule than glucose, both in molecular weight and in topological polar surface area (TPSA), as shown in Table 1. Due to its size, laminarin may contribute to a more substantial organic shell around the sea salt core in mixed sea salt/laminarin/surfactant particles. Under low RH conditions, there may not be sufficient water vapor to adsorb and dissolve the laminarin to the bulk of the particle. If the laminarin and surfactant remain as a particle coating or shell, this could prevent exposure of water vapor to the sea salt core and inhibit particle water uptake.[104] In itself, this may cause a decrease in GF. Second, the dampening of water uptake would thus decrease the electrolyte shielding of ionic surfactants since less water would be present to dissolve and promote dissolution of low DRH salts, such as $MgCl_2$, in sea salt. This could explain why particles containing laminarin and ionic surfactants do not experience the same increase in GF shown and discussed previously for sea salt/glucose/ionic surfactant particles under conditions below the DRH. As a third related factor, the large size of laminarin may compete with the surfactants for space at the particle surface. This would prevent surfactant monolayer coverage at the surface of sea salt/laminarin particles and thus prevent any reduction in particle surface tension that would increase the GF. While laminarin is a large organic molecule that may be surface-active, it is not a strong surfactant and thus has a lesser effect on surface tension.

The sea salt/laminarin/surfactant particles demonstrate less hygroscopic growth and thus have less surface area than the sea salt/glucose/surfactant particles at 70% RH (Figure 2). This means that surfactants in sea salt/laminarin particles would saturate the surface more than surfactants in the larger sea salt/glucose particles at this RH. More surfactant coverage would correspond to a decrease in particle surface tension, which would enhance hygroscopic growth. This could explain why immediately after reaching deliquescence, most sea salt/laminarin/surfactant particles, except those containing SDS or Tergitol, have higher GFs compared to the GFs of sea salt/glucose/surfactant particles right after deliquescence (Table S2). Additional solutes in particles containing surfactants also influence surfactant partitioning to the particle surface.[71] The differences in hygroscopic growth between sea salt/glucose and sea salt/laminarin particles could be caused by changes in surfactant partitioning behavior in the presence of glucose compared to laminarin.

At RHs greater than the DRH, the change in GFs for sea salt/sugar/surfactant particles from those of sea salt/sugar only particles are similar for both glucose and laminarin but vary based on the type of surfactant added. As discussed earlier, both sea salt/laminarin and sea salt/glucose particles demonstrate a decrease in GFs with the addition of anionic and nonionic surfactants when the RH is greater than the DRH. The change in GFs with the addition of cationic surfactants is minimal for both the sea salt/glucose and the sea salt/laminarin particles, with the GFs at 90% RH for both particle types showing slight increases compared to the pure sea salt/sugar particles (Figure 2). The similarity in the trends at high RH, beyond the DRH, indicates that the hygroscopicity of the bulk particle controls the GFs at these particle concentrations. At high RH, the particle water content is high, and the particle solute is diluted, which allows the sugars and surfactants to dissolve. For increasing RH, the particle dilution also contributes to an increase in particle surface tension.[71] As the particle size increases, the particle surface-to-volume ratio decreases, which could prevent full monolayer coverage for the mass ratio of surfactant probed in this study.

https://doi.org/10.1021/acs.jpca.2c04539
J. Phys. Chem. A XXXX, XXX, XXX−XXX

At high RHs and for both sugars, the surfactants contribute to further decreasing the bulk hygroscopicity of sea salt/sugar particles.

The GFs of all sea salt/sugar/surfactant particles at 90% RH show trends with the TPSA of surfactant molecules (Figure 4).

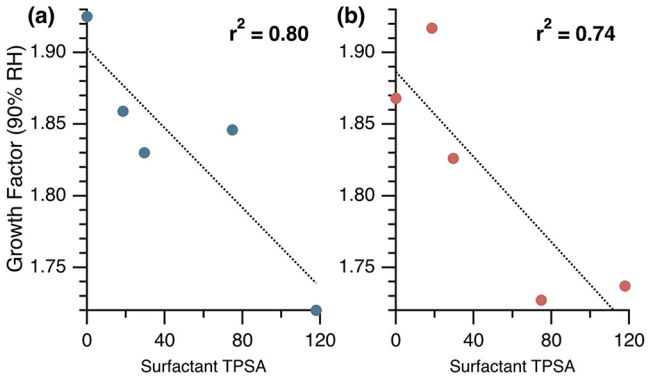

Figure 4. Linear correlation plots of surfactant topological polar surface area (TPSA) and GF at 90% RH for 100 nm (a) sea salt/glucose/surfactant particles and (b) sea salt/laminarin/surfactant particles. Error bars are smaller than the markers on this scale and thus are not included. The standard deviations of the GFs at 90% RH are listed in Table 3.

There is a decrease in the GF at 90% RH with an increase in the surfactant TSPA for both the sea salt/glucose/surfactant particles (r^2 = 0.80) and sea salt/laminarin/surfactant particles (r^2 = 0.74) (Figure 4). TPSA quantifies the molecular surface area of polar atoms, which include nitrogen and oxygen and their attached hydrogen atoms.[112] It has been used previously to describe and predict molecular characteristics such as aqueous solubility and critical micelle concentration (CMC) due to how TPSA relates to molecular polarity and hydrogen-bonding potential.[113] Since TPSA has been tied to solubility and CMC, which are properties that influence particle surface tension and hygroscopic growth, it may have the potential to also predict the influence of the surfactant on hygroscopic growth. This could explain the correlation between the TPSA of the surfactant and the hygroscopic growth of an aqueous sea salt/sugar/surfactant particle. Because the trend in the GFs at 90% RH are similar across particle dry diameters, as discussed in section 3.3, the TPSA has similar correlations with GFs at 90% RH for dry particle diameters of 50 and 300 nm as well. Because TPSA is the surface area of the polar atoms, it is not indicative of total molecule size or the packing efficiency at the surface and thus is not indicative of a reduction in surface tension.

As a particle takes up water, the surface tension will continue to evolve as a function of the water content and chemical concentrations. The CCN activity can increase or decrease depending on the influence of organic compounds on surface tension, which does not remain static but continues to change as the RH increases and hygroscopic growth occurs.[114] This can explain the unique characteristics of the hygroscopic growth curve of each particle composition and how surfactants can change the hygroscopic properties of particles across a wide RH range even when present at low mass fractions.

3.3. Influence of Surfactants on Hygroscopic Growth of Different Sized Particles. In addition to 100 nm diameter particles, the hygroscopic growth of surfactant-containing particles was measured for 50 and 300 nm diameter particles to determine whether the effects of the surfactant on water uptake change with dry particle size. The results shown in Figure 5 exhibit the known dependence of hygroscopic growth (represented by GF) on particle dry diameter.[27] Larger particles have greater hygroscopic growth than smaller particles. At 90% RH, there is an increase in GF for all particle compositions as the particle diameter increases from 50 to 300 nm (Figure 5). This trend is expected and is described by the Kelvin effect in Kohler theory, which takes into account particle surface-to-volume ratio and surface tension.[43] Even though the particle hygroscopic growth varies with particle composition, the increase in water uptake

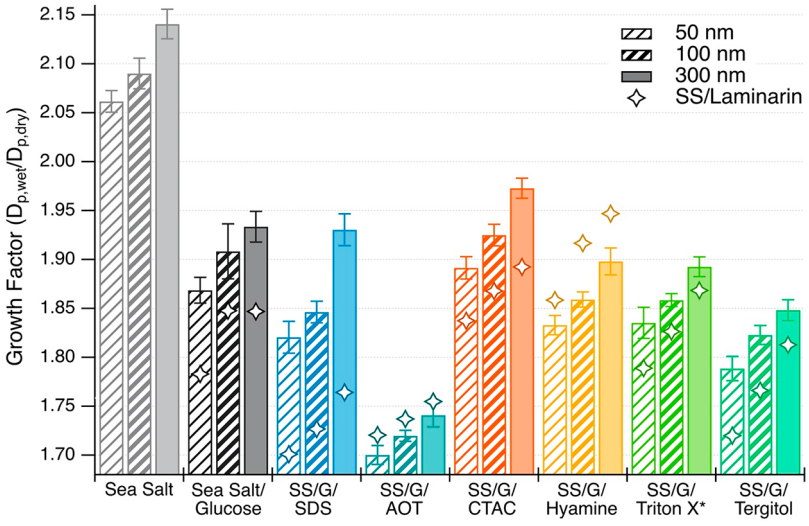

Figure 5. Hygroscopic growth factors at 90% RH (GF_{90}) measured at three dry particle diameters: 50, 100, and 300 nm. Bars represent GFs for sea salt, sea salt/glucose (2:1), and sea salt/glucose/surfactant (SS/G/surfactant) (2:0.9:0.1). The error bars represent the standard deviation of the GFs averaged over four to six HTDMA scans for each configuration. Diamond markers represent the GFs for the same particle diameters and compositional ratios but with laminarin instead of glucose. *The SS/G/Triton X results in this figure at 90% RH correspond to a 2:1:0.1 mass ratio because of inconsistent size results for 2:0.9:0.1 SS/G/Triton X experiments.

https://doi.org/10.1021/acs.jpca.2c04539
J. Phys. Chem. A XXXX, XXX, XXX−XXX

attributed to particle size holds within the different particle compositions (Figure 5).

The increase in GF from one particle size to a larger particle size is not linear, and the extent of this increase varies depending on the particle composition, including differences based on both the sugar and the surfactant present in the particle. For pure sea salt particles, GF_{90} increases 3.8% in going from 50 to 300 nm particles. The addition of glucose to sea salt for 2:1 sea salt/glucose particles causes a smaller growth increase going from 50 to 300 nm particles (3.5%). The effect of surfactants on particle water uptake is dependent on the particle size, as an increase in particle size corresponds to a decrease in particle surface-to-volume ratio.[115] A humidified particle with a dry diameter of 300 nm will therefore have a higher bulk surfactant concentration than a humidified particle with a dry diameter of 50 nm. The effect of surfactants would then change with a change in particle size. This explains the large differences in growth exhibited by surfactant-containing particles compared to sea salt only and sea salt/glucose only particles (Figure 5). For example, from 50 to 300 nm, the GF of sea salt/glucose/AOT particles increases by 2.4%, while for sea salt/glucose/SDS particles the GF increases by 6.0% (Figure 5). The differences between the particles with different surfactants may be attributed to the effect of those surfactants on the hygroscopicity of the particle, as discussed earlier. This may be largely dependent on the size of the surfactant and/or its solubility. Additionally, particles with a greater surfactant monolayer coverage have been shown to require more time to reach equilibration,[116] which could indicate that smaller particles may not have sufficient time to reach equilibrium size. Even though surfactants make up only 3% of the particle composition, each surfactant has its own unique structure, surface activity, and bulk-to-surface partitioning, which would affect the monolayer coverage. This could cause deviations in the growth factor increase observed in going from 50 to 300 nm between different particle compositions.

There are also differences in the extent of the increase in water uptake with particle size when comparing the sea salt/glucose particles to sea salt/laminarin particles, both with and without surfactants (Figure 5). The ratio of GF of 300 nm particles to the GF of 50 nm particles for 90% RH was used to quantify the increase in hygroscopic growth with particle size (Table S3). A larger increase in GF with particle size was observed for anionic surfactants, both SDS and AOT, when present in sea salt/glucose particles, as opposed to sea salt/laminarin particles. Meanwhile, nonionic surfactants, both Triton X and Tergitol, present in sea salt/laminarin particles resulted in a larger increase in GF with particle size than when present in sea salt/glucose particles. For cationic surfactants, the results varied, as CTAC in sea salt/glucose particles showed a larger increase in GF with particle size whereas Hyamine showed a larger increase in GF with particle size when present in sea salt/laminarin particles. These trends in particle size related to surfactants in particles with different organic constituents correspond to the molecular weight of the surfactant (Table 1). The surfactants with the larger molecular weights (Hyamine, Triton X, and Tergitol) caused a more significant increase in GF with particle size when present in sea salt/laminarin particles. At the same time, surfactants with the lower molecular weights (SDS, AOT, and CTAC) caused a larger increase in GF with particle size when present in sea salt/glucose particles. These results point to the importance of understanding the interactions between surfactants and other organic compounds in particles. The composition and complexity of the organic fraction could affect surfactant partitioning, particle surface coverage, solubility, etc. This shows that the interplay of surfactants and other organic compounds in a particle can also determine the extent of increase in hygroscopic growth with increasing particle size.

4. CONCLUSIONS

The differences in the GFs observed with the addition of surfactants to model SSA in the form of sea salt/glucose and sea salt/laminarin particles demonstrate the importance of understanding the full organic composition of SSA particles. Individual organic compounds were shown to contribute to and influence hygroscopic growth in unique ways, further proving that single organic compound proxies cannot serve as sufficient representations of the full organic fraction of SSA. Even though surfactants may be present in lower mass fractions relative to sea salt and other organic compounds in SSA, this study shows that they can significantly alter the hygroscopic properties of SSA. This effect depends on the individual characteristics of the surfactants, including ionicity, chemical structure, and bulk-to-surface partitioning in the presence of other organic compounds.

Alone, at RHs less than the DRH, the addition of glucose does not change the GFs of sea salt particles. However, the presence of an anionic or cationic surfactant increases the GF of sea salt/glucose particles and decreases the DRH. This implies that particles with organic fractions containing both simple sugars and surfactants may have enhanced water uptake, deliquesce at lower RH, and thus have increased CCN potential. The determination of particle CCN potential, however, greatly relies on measuring and considering the particle interfacial tension and how it varies between particle compositions. For particles containing surfactants and more complex sugars, such as laminarin, the surfactants may not play as large a role at RHs less than the DRH. Instead, these surfactants may contribute to the overall decrease in hygroscopicity of sea salt/laminarin particles, as the more complex sugar can hinder surfactant partitioning to the surface of the particles. At RHs greater than the DRH, the addition of anionic and nonionic surfactants to both sea salt/glucose and sea salt/laminarin particles acts to further decrease the particle hygroscopic growth compared to the sea salt/sugar particles alone. While the addition of cationic surfactants causes minimal change in the water uptake of sea salt/sugar particles at high RHs, they show the potential to increase hygroscopic growth. When considering measured surface tensions, the particle CCN potential of inorganic/organic particles increases greatly with the addition of all surfactants, but more notably with ionic surfactants.

Together, these studies indicate the importance of atmospheric measurements of the composition and concentration of the organic fraction of submicrometer aerosol particles, including characterization of the surfactant fraction. Assumptions made about the composition and properties of the organic fraction of the aerosol particles may under- or overestimate the hygroscopic growth. It is critical not only to understand the hygroscopic properties of individual aerosol particle components but also to investigate the hygroscopic properties of mixed particles and the influence of individual constituents on the bulk particle hygroscopicity. Further understanding of particle water uptake becomes more

https://doi.org/10.1021/acs.jpca.2c04539
J. Phys. Chem. A XXXX, XXX, XXX−XXX

important in the size-resolved chemical composition shown in SSA and will be crucial to constraining the CCN activation potential of the range of SSA particle compositions and sizes.

■ ASSOCIATED CONTENT

Supporting Information

The Supporting Information is available free of charge at https://pubs.acs.org/doi/10.1021/acs.jpca.2c04539.

HTDMA number size distributions (Figure S1); experiment configurations (Table S1); GFs as a function of particle organic fraction at different RHs (Figure S2); influence of organic fraction on growth factors (Text S1); GFs as a function of RH for different mixtures of sea salt and glucose (Figure S3); dependence of sea salt/glucose/surfactant (2:0.9:0.1) solutions on surfactant concentration (Figure S4); explanation of the surface tension measurements and their use in calculating hygroscopicity (Text S2); measured surface tension values for each particle composition used in calculating hygroscopicity (Table S2); explanation of the extrapolation of measured surface tension from bulk solution surface tension measurements (Text S3); calculated solute concentrations for each constituent (sea salt, glucose, and surfactant) in 100 nm particles humidified to 90% RH (Table S3); GFs at the DRH of sea salt/glucose and sea salt/laminarin particles with the addition of surfactants (Table S4); ratios of GFs at 300 and 50 nm with the addition of different surfactants (Table S5) (PDF)

■ AUTHOR INFORMATION

Corresponding Author

Amanda A. Frossard − *Department of Chemistry, University of Georgia, Athens, Georgia 30606, United States;* orcid.org/0000-0002-5728-0854; Phone: 706-542-1968; Email: afrossard@uga.edu

Author

Rachel L. Bramblett − *Department of Chemistry, University of Georgia, Athens, Georgia 30606, United States*

Complete contact information is available at: https://pubs.acs.org/10.1021/acs.jpca.2c04539

Author Contributions

The manuscript was written through contributions of all authors. All of the authors approved the final version of the manuscript.

Funding

This material is based upon work supported by the University of Georgia Investment in Sciences Initiative and Office of Research. Further support was provided by the University of Georgia 2019 Presidential Seed Grant.

Notes

The authors declare no competing financial interest.

■ ACKNOWLEDGMENTS

The authors thank Dr. Fred J. Brechtel at Brechtel Manufacturing Inc. (BMI) for his insight and assistance with the HTDMA and data analyses.

■ REFERENCES

(1) Lewis, E. R.; Schwartz, S. E.*Sea Salt Aerosol Production: Mechanisms, Methods, Measurements, and Models*; American Geophysical Union, 2004.

(2) de Leeuw, G.; Andreas, E. L.; Anguelova, M. D.; Fairall, C.; Lewis, E. R.; O'Dowd, C.; Schulz, M.; Schwartz, S. E. Production flux of sea spray aerosol. *Rev. Geophys.* **2011**, *49* (2), RG2001.

(3) Engel, A.; Bange, H. W.; Cunliffe, M.; Burrows, S. M.; Friedrichs, G.; Galgani, L.; Herrmann, H.; Hertkorn, N.; Johnson, M.; Liss, P. S.; et al. The ocean's vital skin: Toward an integrated understanding of the sea surface microlayer. *Front. Mar. Sci.* **2017**, *4*, 165.

(4) O'Dowd, C. D.; De Leeuw, G. Marine aerosol production: a review of the current knowledge. *Philos. Trans. R. Soc. A.* **2007**, *365* (1856), 1753−1774.

(5) Gong, S. L.; Barrie, L. A.; Lazare, M. Canadian Aerosol Module (CAM): A size-segregated simulation of atmospheric aerosol processes for climate and air quality models 2. Global sea-salt aerosol and its budgets. *J. Geophys. Res.: Atmos.* **2002**, *107* (D24), AAC 13-1−AAC 13-14.

(6) Resch, F.; Darrozes, J.; Afeti, G. Marine liquid aerosol production from bursting of air bubbles. *J. Geophys. Res.: Oceans* **1986**, *91* (C1), 1019−1029.

(7) Spiel, D. E. On the births of film drops from bubbles bursting on seawater surfaces. *J. Geophys. Res.: Oceans* **1998**, *103* (C11), 24907−24918.

(8) Su, B.; Wang, T.; Zhang, G.; Liang, Y.; Lv, C.; Hu, Y.; Li, L.; Zhou, Z.; Wang, X.; Bi, X. A review of atmospheric aging of sea spray aerosols: Potential factors affecting chloride depletion. *Atmos. Environ.* **2022**, *290*, 119365.

(9) Rossi, M. J. Heterogeneous reactions on salts. *Chem. Rev.* **2003**, *103* (12), 4823−4882.

(10) Ammann, M.; Cox, R. A.; Crowley, J.; Jenkin, M. E.; Mellouki, A.; Rossi, M. J.; Troe, J.; Wallington, T. J. Evaluated kinetic and photochemical data for atmospheric chemistry: Volume VI−heterogeneous reactions with liquid substrates. *Atmos. Chem. Phys.* **2013**, *13* (16), 8045−8228.

(11) Yao, X.; Zhang, L. Chemical processes in sea-salt chloride depletion observed at a Canadian rural coastal site. *Atmos. Environ.* **2012**, *46*, 189−194.

(12) Zhou, X.; Davis, A. J.; Kieber, D. J.; Keene, W. C.; Maben, J. R.; Maring, H.; Dahl, E. E.; Izaguirre, M. A.; Sander, R.; Smoydzyn, L. Photochemical production of hydroxyl radical and hydroperoxides in water extracts of nascent marine aerosols produced by bursting bubbles from Sargasso seawater. *Geophys. Res. Lett.* **2008**, *35* (20), L20803.

(13) Turekian, V. C.; Macko, S. A.; Keene, W. C. Concentrations, isotopic compositions, and sources of size-resolved, particulate organic carbon and oxalate in near-surface marine air at Bermuda during spring. *J. Geophys. Res.: Atmos.* **2003**, *108* (D5), 4157.

(14) King, S. M.; Butcher, A. C.; Rosenoern, T.; Coz, E.; Lieke, K. I.; De Leeuw, G.; Nilsson, E. D.; Bilde, M. Investigating primary marine aerosol properties: CCN activity of sea salt and mixed inorganic−organic particles. *Environ. Sci. Technol.* **2012**, *46* (19), 10405−10412.

(15) Randles, C. A.; Russell, L. M.; Ramaswamy, V. Hygroscopic and optical properties of organic sea salt aerosol and consequences for climate forcing. *Geophys. Res. Lett.* **2004**, *31* (16), L16108.

(16) O'Dowd, C. D.; Smith, M. H.; Consterdine, I. E.; Lowe, J. A. Marine aerosol, sea-salt, and the marine sulphur cycle: A short review. *Atmos. Environ.* **1997**, *31* (1), 73−80.

(17) Twomey, S. The influence of pollution on the shortwave albedo of clouds. *J. Atmos. Sci.* **1977**, *34*, 1149−1152.

(18) Garrett, T. J.; Radke, L. F.; Hobbs, P. V. Aerosol effects on cloud emissivity and surface longwave heating in the Arctic. *J. Atmos. Sci.* **2002**, *59* (3), 769−778.

(19) McFiggans, G.; Artaxo, P.; Baltensperger, U.; Coe, H.; Facchini, M. C.; Feingold, G.; Fuzzi, S.; Gysel, M.; Laaksonen, A.; Lohmann, U.; et al. The effect of physical and chemical aerosol properties on warm cloud droplet activation. *Atmos. Chem. Phys.* **2006**, *6* (9), 2593−2649.

(20) Weis, D. D.; Ewing, G. E. The reaction of nitrogen dioxide with sea salt aerosol. *J. Phys. Chem. A* **1999**, *103* (25), 4865−4873.
(21) Spurny, K. R.*Aerosol Chemical Processes in the Environment*; CRC Press, 2000.
(22) Edgar, G.; Swan, W. O. The factors determining the hygroscopic properties of soluble substances. I. The vapor pressures of saturated solutions. *J. Am. Chem. Soc.* **1922**, *44* (3), 570−577.
(23) Zieger, P.; Väisänen, O.; Corbin, J. C.; Partridge, D. G.; Bastelberger, S.; Mousavi-Fard, M.; Rosati, B.; Gysel, M.; Krieger, U. K.; Leck, C.; et al. Revising the hygroscopicity of inorganic sea salt particles. *Nat. Commun.* **2017**, *8* (1), 15883.
(24) Winkler, P. The growth of atmospheric aerosol particles as a function of the relative humidity—II. An improved concept of mixed nuclei. *J. Aerosol Sci.* **1973**, *4* (5), 373−387.
(25) O'Dowd, C. D.; Facchini, M. C.; Cavalli, F.; Ceburnis, D.; Mircea, M.; Decesari, S.; Fuzzi, S.; Yoon, Y. J.; Putaud, J.-P. Biogenically driven organic contribution to marine aerosol. *Nature* **2004**, *431* (7009), 676−680.
(26) Prather, K. A.; Bertram, T. H.; Grassian, V. H.; Deane, G. B.; Stokes, M. D.; DeMott, P. J.; Aluwihare, L. I.; Palenik, B. P.; Azam, F.; Seinfeld, J. H.; et al. Bringing the ocean into the laboratory to probe the chemical complexity of sea spray aerosol. *Proc. Natl. Acad. Sci. U. S. A.* **2013**, *110* (19), 7550−7555.
(27) Laskina, O.; Morris, H. S.; Grandquist, J. R.; Qin, Z.; Stone, E. A.; Tivanski, A. V.; Grassian, V. H. Size matters in the water uptake and hygroscopic growth of atmospherically relevant multicomponent aerosol particles. *J. Phys. Chem. A* **2015**, *119* (19), 4489−4497.
(28) Lei, T.; Zuend, A.; Wang, W.; Zhang, Y.; Ge, M. Hygroscopicity of organic compounds from biomass burning and their influence on the water uptake of mixed organic ammonium sulfate aerosols. *Atmos. Chem. Phys.* **2014**, *14* (20), 11165−11183.
(29) Harmon, C. W.; Grimm, R. L.; McIntire, T. M.; Peterson, M. D.; Njegic, B.; Angel, V. M.; Alshawa, A.; Underwood, J. S.; Tobias, D. J.; Gerber, R. B.; et al. Hygroscopic growth and deliquescence of NaCl nanoparticles mixed with surfactant SDS. *J. Phys. Chem. B* **2010**, *114* (7), 2435−2449.
(30) Peng, C.; Chow, A. H.; Chan, C. K. Hygroscopic study of glucose, citric acid, and sorbitol using an electrodynamic balance: Comparison with UNIFAC predictions. *Aerosol Sci. Technol.* **2001**, *35* (3), 753−758.
(31) Mochida, M.; Kawamura, K. Hygroscopic properties of levoglucosan and related organic compounds characteristic to biomass burning aerosol particles. *J. Geophys. Res.: Atmos.* **2004**, *109* (D21), D21202.
(32) Tang, I. N.; Tridico, A.; Fung, K. Thermodynamic and optical properties of sea salt aerosols. *J. Geophys. Res.: Atmos.* **1997**, *102* (D19), 23269−23275.
(33) Frossard, A. A.; Russell, L. M.; Burrows, S. M.; Elliott, S. M.; Bates, T. S.; Quinn, P. K. Sources and composition of submicron organic mass in marine aerosol particles. *J. Geophys. Res.: Atmos.* **2014**, *119* (22), 12977−13003.
(34) Quinn, P. K.; Bates, T. S.; Schulz, K. S.; Coffman, D.; Frossard, A.; Russell, L.; Keene, W.; Kieber, D. Contribution of sea surface carbon pool to organic matter enrichment in sea spray aerosol. *Nat. Geosci.* **2014**, *7* (3), 228−232.
(35) Cochran, R. E.; Laskina, O.; Trueblood, J. V.; Estillore, A. D.; Morris, H. S.; Jayarathne, T.; Sultana, C. M.; Lee, C.; Lin, P.; Laskin, J.; et al. Molecular diversity of sea spray aerosol particles: Impact of ocean biology on particle composition and hygroscopicity. *Chem* **2017**, *2* (5), 655−667.
(36) *Climate Change 2013: The Physical Science Basis. Contribution of Working Group I to the Fifth Assessment Report of the Intergovernmental Panel on Climate Change*; Stocker, T. F., Qin, D., Plattner, G.-K., Tignor, M., Allen, S. K., Boschung, J., Nauels, A., Xia, Y., Bex, V., Midgley, P. M., Eds.; Cambridge University Press, 2013.
(37) Textor, C.; Schulz, M.; Guibert, S.; Kinne, S.; Balkanski, Y.; Bauer, S.; Berntsen, T.; Berglen, T.; Boucher, O.; Chin, M.; et al. Analysis and quantification of the diversities of aerosol life cycles within AeroCom. *Atmos. Chem. Phys.* **2006**, *6* (7), 1777−1813.
(38) Guo, L.; Gu, W.; Peng, C.; Wang, W.; Li, Y. J.; Zong, T.; Tang, Y.; Wu, Z.; Lin, Q.; Ge, M.; et al. A comprehensive study of hygroscopic properties of calcium-and magnesium-containing salts: implication for hygroscopicity of mineral dust and sea salt aerosols. *Atmos. Chem. Phys.* **2019**, *19* (4), 2115−2133.
(39) Choi, M. Y.; Chan, C. K. The effects of organic species on the hygroscopic behaviors of inorganic aerosols. *Environ. Sci. Technol.* **2002**, *36* (11), 2422−2428.
(40) Wu, J.; Faccinetto, A.; Grimonprez, S.; Batut, S.; Yon, J.; Desgroux, P.; Petitprez, D. Influence of the dry aerosol particle size distribution and morphology on the cloud condensation nuclei activation. An experimental and theoretical investigation. *Atmos. Chem. Phys.* **2020**, *20* (7), 4209−4225.
(41) Ruehl, C. R.; Wilson, K. R. Surface organic monolayers control the hygroscopic growth of submicrometer particles at high relative humidity. *J. Phys. Chem. A* **2014**, *118* (22), 3952−3966.
(42) Frossard, A. A.; Li, W.; Gérard, V.; Nozière, B.; Cohen, R. C. Influence of surfactants on growth of individual aqueous coarse mode aerosol particles. *Aerosol Sci. Technol.* **2018**, *52* (4), 459−469.
(43) Köhler, H. The nucleus in and the growth of hygroscopic droplets. *Trans. Faraday Soc.* **1936**, *32*, 1152−1161.
(44) Shulman, M. L.; Jacobson, M. C.; Carlson, R. J.; Synovec, R. E.; Young, T. E. Dissolution behavior and surface tension effects of organic compounds in nucleating cloud droplets. *Geophys. Res. Lett.* **1996**, *23* (3), 277−280.
(45) Petters, M. D.; Kreidenweis, S. A single parameter representation of hygroscopic growth and cloud condensation nucleus activity. *Atmos. Chem. Phys.* **2007**, *7* (8), 1961−1971.
(46) Wex, H.; Stratmann, F.; Topping, D.; McFiggans, G. The Kelvin versus the Raoult term in the Köhler equation. *J. Atmos. Sci.* **2008**, *65* (12), 4004−4016.
(47) Saxena, P.; Hildemann, L. M.; McMurry, P. H.; Seinfeld, J. H. Organics alter hygroscopic behavior of atmospheric particles. *J. Geophys. Res.: Atmos.* **1995**, *100* (D9), 18755−18770.
(48) Ming, Y.; Russell, L. M. Predicted hygroscopic growth of sea salt aerosol. *J. Geophys. Res.: Atmos.* **2001**, *106* (D22), 28259−28274.
(49) Xu, W.; Ovadnevaite, J.; Fossum, K. N.; Lin, C.; Huang, R. J.; O'Dowd, C.; Ceburnis, D. Aerosol hygroscopicity and its link to chemical composition in the coastal atmosphere of Mace Head: marine and continental air masses. *Atmos. Chem. Phys.* **2020**, *20* (6), 3777−3791.
(50) Wang, Y.; Jing, B.; Guo, Y.; Li, J.; Tong, S.; Zhang, Y.; Ge, M. Water uptake of multicomponent organic mixtures and their influence on hygroscopicity of inorganic salts. *J. Environ. Sci.* **2016**, *45*, 156−163.
(51) Holmgren, H.; Sellegri, K.; Hervo, M.; Rose, C.; Freney, E.; Villani, P.; Laj, P. Hygroscopic properties and mixing state of aerosol measured at the high-altitude site Puy de Dôme (1465 m asl), France. *Atmos. Chem. Phys.* **2014**, *14* (18), 9537−9554.
(52) Cruz, C. N.; Pandis, S. N. Deliquescence and hygroscopic growth of mixed inorganic− organic atmospheric aerosol. *Environ. Sci. Technol.* **2000**, *34* (20), 4313−4319.
(53) Hämeri, K.; Laaksonen, A.; Väkevä, M.; Suni, T. Hygroscopic growth of ultrafine sodium chloride particles. *J. Geophys. Res.: Atmos.* **2001**, *106* (D18), 20749−20757.
(54) Bates, T.; Quinn, P.; Frossard, A.; Russell, L.; Hakala, J.; Petäjä, T.; Kulmala, M.; Covert, D.; Cappa, C.; Li, S. M. Measurements of ocean derived aerosol off the coast of California. *J. Geophys. Res.: Atmos.* **2012**, *117* (D21), D00V15.
(55) Quinn, P. K.; Collins, D. B.; Grassian, V. H.; Prather, K. A.; Bates, T. S. Chemistry and related properties of freshly emitted sea spray aerosol. *Chem. Rev.* **2015**, *115* (10), 4383−4399.
(56) Zhang, X.; Massoli, P.; Quinn, P. K.; Bates, T. S.; Cappa, C. D. Hygroscopic growth of submicron and supermicron aerosols in the marine boundary layer. *J. Geophys. Res.: Atmos.* **2014**, *119* (13), 8384−8399.
(57) Niedermeier, D.; Wex, H.; Voigtländer, J.; Stratmann, F.; Brüggemann, E.; Kiselev, A.; Henk, H.; Heintzenberg, J. LACIS-

https://doi.org/10.1021/acs.jpca.2c04539
J. Phys. Chem. A XXXX, XXX, XXX−XXX

measurements and parameterization of sea-salt particle hygroscopic growth and activation. *Atmos. Chem. Phys.* **2008**, *8* (3), 579−590.
(58) Kristensen, T. B.; Prisle, N. L.; Bilde, M. Cloud droplet activation of mixed model HULIS and NaCl particles: Experimental results and κ-Köhler theory. *Atmos. Res.* **2014**, *137*, 167−175.
(59) Ren, J.; Zhang, F.; Wang, Y.; Collins, D.; Fan, X.; Jin, X.; Xu, W.; Sun, Y.; Cribb, M.; Li, Z. Using different assumptions of aerosol mixing state and chemical composition to predict CCN concentrations based on field measurements in urban Beijing. *Atmos. Chem. Phys.* **2018**, *18* (9), 6907−6921.
(60) Hendrickson, B. N.; Brooks, S. D.; Thornton, D. C.; Moore, R. H.; Crosbie, E.; Ziemba, L. D.; Carlson, C. A.; Baetge, N.; Mirrielees, J. A.; Alsante, A. N. Role of sea surface microlayer properties in cloud formation. *Front. Mar. Sci.* **2021**, *7*, 596225.
(61) Clegg, S. L.; Brimblecombe, P.; Wexler, A. S. Thermodynamic model of the system H^+−NH_4^+−Na^+−SO_4^{2-}−NO_3^-−Cl^-−H_2O at 298.15 K. *J. Phys. Chem. A* **1998**, *102* (12), 2155−2171.
(62) Liu, P.; Song, M.; Zhao, T.; Gunthe, S. S.; Ham, S.; He, Y.; Qin, Y. M.; Gong, Z.; Amorim, J. C.; Bertram, A. K.; et al. Resolving the mechanisms of hygroscopic growth and cloud condensation nuclei activity for organic particulate matter. *Nat. Commun.* **2018**, *9* (1), 4076.
(63) Forestieri, S. D.; Staudt, S. M.; Kuborn, T. M.; Faber, K.; Ruehl, C. R.; Bertram, T. H.; Cappa, C. D. Establishing the impact of model surfactants on cloud condensation nuclei activity of sea spray aerosol mimics. *Atmos. Chem. Phys.* **2018**, *18* (15), 10985−11005.
(64) Petters, S. S.; Petters, M. D. Surfactant effect on cloud condensation nuclei for two-component internally mixed aerosols. *J. Geophys. Res.: Atmos.* **2016**, *121* (4), 1878−1895.
(65) Ovadnevaite, J.; Zuend, A.; Laaksonen, A.; Sanchez, K. J.; Roberts, G.; Ceburnis, D.; Decesari, S.; Rinaldi, M.; Hodas, N.; Facchini, M. C.; et al. Surface tension prevails over solute effect in organic-influenced cloud droplet activation. *Nature* **2017**, *546* (7660), 637−641.
(66) Frossard, A. A.; Gérard, V.; Duplessis, P.; Kinsey, J. D.; Lu, X.; Zhu, Y.; Bisgrove, J.; Maben, J. R.; Long, M. S.; Chang, R. Y.-W.; et al. Properties of seawater surfactants associated with primary marine aerosol particles produced by bursting bubbles at a model air−sea interface. *Environ. Sci. Technol.* **2019**, *53* (16), 9407−9417.
(67) Gerard, V.; Noziere, B.; Baduel, C.; Fine, L.; Frossard, A. A.; Cohen, R. C. Anionic, cationic, and nonionic surfactants in atmospheric aerosols from the baltic coast at askö, sweden: Implications for cloud droplet activation. *Environ. Sci. Technol.* **2016**, *50* (6), 2974−2982.
(68) Cavalli, F.; Facchini, M.; Decesari, S.; Mircea, M.; Emblico, L.; Fuzzi, S.; Ceburnis, D.; Yoon, Y.; O'Dowd, C.; Putaud, J. P.; et al. Advances in characterization of size-resolved organic matter in marine aerosol over the North Atlantic. *J. Geophys. Res.: Atmos.* **2004**, *109* (D24), D24215.
(69) Facchini, M. C.; Rinaldi, M.; Decesari, S.; Carbone, C.; Finessi, E.; Mircea, M.; Fuzzi, S.; Ceburnis, D.; Flanagan, R.; Nilsson, E. D.; et al. Primary submicron marine aerosol dominated by insoluble organic colloids and aggregates. *Geophys. Res. Lett.* **2008**, *35* (17), L17814.
(70) Wokosin, K. A.; Schell, E. L.; Faust, J. A. Surfactants, Films, and Coatings on Atmospheric Aerosol Particles: A Review. *Environ. Sci.: Atmos.* **2022**, *2* (5), 775−828.
(71) Bzdek, B. R.; Reid, J. P.; Malila, J.; Prisle, N. L. The surface tension of surfactant-containing, finite volume droplets. *Proc. Natl. Acad. Sci. U. S. A.* **2020**, *117* (15), 8335−8343.
(72) Keene, W. C.; Maring, H.; Maben, J. R.; Kieber, D. J.; Pszenny, A. A. P.; Dahl, E. E.; Izaguirre, M. A.; Davis, A. J.; Long, M. S.; Zhou, X.; et al. Chemical and physical characteristics of nascent aerosols produced by bursting bubbles at a model air-sea interface. *J. Geophys. Res.: Atmos.* **2007**, *112* (D21), D21202.
(73) Vaccaro, R. F.; Hicks, S. E.; Jannasch, H. W.; Carey, F. G. The occurrence and role of glucose in seawater. *Limnol. Oceanogr.* **1968**, *13* (2), 356−360.
(74) Miyazaki, Y.; Yamashita, Y.; Kawana, K.; Tachibana, E.; Kagami, S.; Mochida, M.; Suzuki, K.; Nishioka, J. Chemical transfer of dissolved organic matter from surface seawater to sea spray water-soluble organic aerosol in the marine atmosphere. *Sci. Rep* **2018**, *8* (1), 14861.
(75) Becker, S.; Tebben, J.; Coffinet, S.; Wiltshire, K.; Iversen, M. H.; Harder, T.; Hinrichs, K.-U.; Hehemann, J.-H. Laminarin is a major molecule in the marine carbon cycle. *Proc. Natl. Acad. Sci. U. S. A.* **2020**, *117* (12), 6599−6607.
(76) Painter, T. J. Algal polysaccharides. *Polysaccharides* **1983**, 195−285.
(77) Lopez-Yglesias, X. F.; Yeung, M. C.; Dey, S. E.; Brechtel, F. J.; Chan, C. K. Performance evaluation of the Brechtel Mfg. Humidified Tandem Differential Mobility Analyzer (BMI HTDMA) for studying hygroscopic properties of aerosol particles. *Aerosol Sci. Technol.* **2014**, *48* (9), 969−980.
(78) Flagan, R. C. On differential mobility analyzer resolution. *Aerosol Sci. Technol.* **1999**, *30* (6), 556−570.
(79) Wexler, A. S.; Seinfeld, J. H. Second-generation inorganic aerosol model. *Atmos. Environ., Part A* **1991**, *25* (12), 2731−2748.
(80) Petters, M.; Kreidenweis, S. A single parameter representation of hygroscopic growth and cloud condensation nucleus activity. *Atmos. Chem. Phys.* **2007**, *7* (8), 1961−1971.
(81) Cheung, H. H.; Yeung, M. C.; Li, Y. J.; Lee, B. P.; Chan, C. K. Relative humidity-dependent HTDMA measurements of ambient aerosols at the HKUST supersite in Hong Kong, China. *Aerosol Sci. Technol.* **2015**, *49* (8), 643−654.
(82) Petters, M.; Kreidenweis, S. A single parameter representation of hygroscopic growth and cloud condensation nucleus activity−Part 3: Including surfactant partitioning. *Atmos. Chem. Phys.* **2013**, *13* (2), 1081−1091.
(83) Gupta, D.; Kim, H.; Park, G.; Li, X.; Eom, H.-J.; Ro, C.-U. Hygroscopic properties of NaCl and NaNO 3 mixture particles as reacted inorganic sea-salt aerosol surrogates. *Atmos. Chem. Phys.* **2015**, *15* (6), 3379−3393.
(84) Cziczo, D.; Nowak, J.; Hu, J.; Abbatt, J. Infrared spectroscopy of model tropospheric aerosols as a function of relative humidity: Observation of deliquescence and crystallization. *J. Geophys. Res.: Atmos.* **1997**, *102* (D15), 18843−18850.
(85) Cziczo, D.; Abbatt, J. Infrared observations of the response of NaCl, $MgCl_2$, NH_4HSO_4, and NH_4NO_3 aerosols to changes in relative humidity from 298 to 238 K. *J. Phys. Chem. A* **2000**, *104* (10), 2038−2047.
(86) Casillas-Ituarte, N. N.; Callahan, K. M.; Tang, C. Y.; Chen, X.; Roeselová, M.; Tobias, D. J.; Allen, H. C. Surface organization of aqueous MgCl2 and application to atmospheric marine aerosol chemistry. *Proc. Natl. Acad. Sci. U. S. A.* **2010**, *107* (15), 6616−6621.
(87) Tang, I. N. Thermodynamic and optical properties of mixed-salt aerosols of atmospheric importance. *J. Geophys. Res.: Atmos.* **1997**, *102* (D2), 1883−1893.
(88) Gu, W.; Li, Y.; Zhu, J.; Jia, X.; Lin, Q.; Zhang, G.; Ding, X.; Song, W.; Bi, X.; Wang, X.; et al. Investigation of water adsorption and hygroscopicity of atmospherically relevant particles using a commercial vapor sorption analyzer. *Atmos. Meas. Technol.* **2017**, *10* (10), 3821−3832.
(89) Lin, J. J.; Raj R, K.; Wang, S.; Kokkonen, E.; Mikkelä, M.-H.; Urpelainen, S.; Prisle, N. L. Pre-deliquescent water uptake in deposited nanoparticles observed with in situ ambient pressure X-ray photoelectron spectroscopy. *Atmos. Chem. Phys.* **2021**, *21* (6), 4709−4727.
(90) Allen, H. C.; Casillas-Ituarte, N. N.; Sierra-Hernandez, M. R.; Chen, X.; Tang, C. Y. Shedding light on water structure at air−aqueous interfaces: ions, lipids, and hydration. *Phys. Chem. Chem. Phys.* **2009**, *11* (27), 5538−5549.
(91) Bryan, C. R.; Knight, A. W.; Katona, R. M.; Sanchez, A.; Schindelholz, E. J.; Schaller, R. F. Physical and chemical properties of sea salt deliquescent brines as a function of temperature and relative humidity. *Sci. Total Environ.* **2022**, *824*, 154462.

https://doi.org/10.1021/acs.jpca.2c04539
J. Phys. Chem. A XXXX, XXX, XXX−XXX

(92) Suda, S. R.; Petters, M. D. Accurate determination of aerosol activity coefficients at relative humidities up to 99% using the hygroscopicity tandem differential mobility analyzer technique. *Aerosol Sci. Technol.* **2013**, *47* (9), 991−1000.
(93) Han, S.; Hong, J.; Luo, Q.; Xu, H.; Tan, H.; Wang, Q.; Tao, J.; Zhou, Y.; Peng, L.; He, Y.; et al. Hygroscopicity of organic compounds as a function of organic functionality, water solubility, molecular weight, and oxidation level. *Atmos. Chem. Phys.* **2022**, *22* (6), 3985−4004.
(94) Mikhailov, E. F.; Vlasenko, S. S. High-humidity tandem differential mobility analyzer for accurate determination of aerosol hygroscopic growth, microstructure, and activity coefficients over a wide range of relative humidity. *Atmos. Meas. Technol.* **2020**, *13* (4), 2035−2056.
(95) Prisle, N. L.; Raatikainen, T.; Sorjamaa, R.; Svenningsson, B.; Laaksonen, A.; Bilde, M. Surfactant partitioning in cloud droplet activation: a study of C8, C10, C12 and C14 normal fatty acid sodium salts. *Tellus B* **2008**, *60* (3), 416−431.
(96) Chen, Y.-Y.; Lee, W.-M. G. The effect of surfactants on the deliquescence of sodium chloride. *J. Environ. Sci. Health, Part A* **2001**, *36* (2), 229−242.
(97) Alshawa, A.; Dopfer, O.; Harmon, C. W.; Nizkorodov, S. A.; Underwood, J. S. Hygroscopic growth and deliquescence of NaCl nanoparticles coated with surfactant AOT. *J. Phys. Chem. A* **2009**, *113* (26), 7678−7686.
(98) Woods, E., III; Kim, H. S.; Wivagg, C. N.; Dotson, S. J.; Broekhuizen, K. E.; Frohardt, E. F. Phase transitions and surface morphology of surfactant-coated aerosol particles. *J. Phys. Chem. A* **2007**, *111* (43), 11013−11020.
(99) Estillore, A. D.; Morris, H. S.; Or, V. W.; Lee, H. D.; Alves, M. R.; Marciano, M. A.; Laskina, O.; Qin, Z.; Tivanski, A. V.; Grassian, V. H. Linking hygroscopicity and the surface microstructure of model inorganic salts, simple and complex carbohydrates, and authentic sea spray aerosol particles. *Phys. Chem. Chem. Phys.* **2017**, *19* (31), 21101−21111.
(100) Zakrzewska, M. E.; Bogel-Łukasik, E.; Bogel-Łukasik, R. Solubility of carbohydrates in ionic liquids. *Energy Fuels* **2010**, *24* (2), 737−745.
(101) Carrero-Carralero, C.; Ruiz-Aceituno, L.; Ramos, L.; Moreno, F. J.; Sanz, M. L. Influence of chemical structure on the solubility of low molecular weight carbohydrates in room temperature ionic liquids. *Ind. Eng. Chem. Res.* **2014**, *53* (36), 13843−13850.
(102) Shamjad, P.; Tripathi, S.; Aggarwal, S.; Mishra, S.; Joshi, M.; Khan, A.; Sapra, B.; Ram, K. Comparison of experimental and modeled absorption enhancement by black carbon (BC) cored polydisperse aerosols under hygroscopic conditions. *Environ. Sci. Technol.* **2012**, *46* (15), 8082−8089.
(103) Chan, M. N.; Lee, A. K.; Chan, C. K. Responses of ammonium sulfate particles coated with glutaric acid to cyclic changes in relative humidity: Hygroscopicity and Raman characterization. *Environ. Sci. Technol.* **2006**, *40* (22), 6983−6989.
(104) Li, W.; Teng, X.; Chen, X.; Liu, L.; Xu, L.; Zhang, J.; Wang, Y.; Zhang, Y.; Shi, Z. Organic coating reduces hygroscopic growth of phase-separated aerosol particles. *Environ. Sci. Technol.* **2021**, *55* (24), 16339−16346.
(105) Prisle, N. L.; Raatikainen, T.; Laaksonen, A.; Bilde, M. Surfactants in cloud droplet activation: mixed organic-inorganic particles. *Atmos. Chem. Phys.* **2010**, *10* (12), 5663−5683.
(106) Moore, M. J.; Furutani, H.; Roberts, G. C.; Moffet, R. C.; Gilles, M. K.; Palenik, B.; Prather, K. A. Effect of organic compounds on cloud condensation nuclei (CCN) activity of sea spray aerosol produced by bubble bursting. *Atmos. Environ.* **2011**, *45* (39), 7462−7469.
(107) Qazi, M. J.; Liefferink, R. W.; Schlegel, S. J.; Backus, E. H.; Bonn, D.; Shahidzadeh, N. Influence of surfactants on sodium chloride crystallization in confinement. *Langmuir* **2017**, *33* (17), 4260−4268.
(108) Goodarzi, F.; Zendehboudi, S. Effects of salt and surfactant on interfacial characteristics of water/oil systems: molecular dynamic simulations and dissipative particle dynamics. *Ind. Eng. Chem. Res.* **2019**, *58* (20), 8817−8834.
(109) Rosen, M. J.; Kunjappu, J. T.*Surfactants and Interfacial Phenomena*; John Wiley & Sons, 2012.
(110) Rekvig, L.; Kranenburg, M.; Hafskjold, B.; Smit, B. Effect of surfactant structure on interfacial properties. *EPL* **2003**, *63* (6), 902.
(111) Kumar, S.; Mandal, A. Studies on interfacial behavior and wettability change phenomena by ionic and nonionic surfactants in presence of alkalis and salt for enhanced oil recovery. *Appl. Surf. Sci.* **2016**, *372*, 42−51.
(112) Prasanna, S.; Doerksen, R. Topological polar surface area: a useful descriptor in 2D-QSAR. *Curr. Med. Chem.* **2009**, *16* (1), 21−41.
(113) Ertl, P.Polar surface area. In *Molecular Drug Properties: Measurement and Prediction*; Mannhold, R., Ed.; Wiley-VCH, 2007; Chapter 5, pp 111−126..
(114) Davies, J. F.; Zuend, A.; Wilson, K. R. The role of evolving surface tension in the formation of cloud droplets. *Atmos. Chem. Phys.* **2019**, *19* (5), 2933−2946.
(115) Sorjamaa, R.; Svenningsson, B.; Raatikainen, T.; Henning, S.; Bilde, M.; Laaksonen, A. The role of surfactants in Köhler theory reconsidered. *Atmos. Chem. Phys.* **2004**, *4* (8), 2107−2117.
(116) Andrews, E.; Larson, S. M. Effect of surfactant layers on the size changes of aerosol particles as a function of relative humidity. *Environ. Sci. Technol.* **1993**, *27* (5), 857−865.
(117) Smith, A. J.; Graves, B.; Child, R.; Rice, P. J.; Ma, Z.; Lowman, D. W.; Ensley, H. E.; Ryter, K. T.; Evans, J. T.; Williams, D. L. Immunoregulatory activity of the natural product laminarin varies widely as a result of its physical properties. *J. Immunol.* **2018**, *200* (2), 788−799.
(118) Hentati, F.; Tounsi, L.; Djomdi, D.; Pierre, G.; Delattre, C.; Ursu, A. V.; Fendri, I.; Abdelkafi, S.; Michaud, P. Bioactive polysaccharides from seaweeds. *Molecules* **2020**, *25* (14), 3152.
(119) Kim, S.; Chen, J.; Cheng, T.; Gindulyte, A.; He, J.; He, S.; Li, Q.; Shoemaker, B. A.; Thiessen, P. A.; Yu, B.; et al. PubChem in 2021: new data content and improved web interfaces. *Nucleic Acids Res.* **2021**, *49* (D1), D1388−D1395.
(120) Lewis, K. A.; Tzilivakis, J.; Warner, D. J.; Green, A. An international database for pesticide risk assessments and management. *Hum. Ecol. Risk Assess.* **2016**, *22* (4), 1050−1064.
(121) Wise, M. E.; Semeniuk, T. A.; Bruintjes, R.; Martin, S. T.; Russell, L. M.; Buseck, P. R. Hygroscopic behavior of NaCl-bearing natural aerosol particles using environmental transmission electron microscopy. *J. Geophys. Res.: Atmos.* **2007**, *112* (D10), D10224.
(122) Peng, C.; Chen, L.; Tang, M. A database for deliquescence and efflorescence relative humidities of compounds with atmospheric relevance. *Fundam. Res.* **2022**, *2* (4), 578−587.
(123) Christensen, S. I.; Petters, M. The role of temperature in cloud droplet activation. *J. Phys. Chem. A* **2012**, *116* (39), 9706−9717.

https://doi.org/10.1021/acs.jpca.2c04539
J. Phys. Chem. A XXXX, XXX, XXX−XXX